AFRL-SR-AR-TR-04-

REPORT DOCUMENTATION PAGE

0455

1. AGENCY USE ONLY (Leave blank)	2. REPORT DATE	3. REPORT TYPE AND DATES COVERED
	July 2004	Final Report January 1,2001-December 31,2003

4. TITLE AND SUBTITLE
New Class of High Temperature Pseudo-Amorphous Oxide Materials

5. FUNDING NUMBERS
F49620-01-C-0014

6. AUTHOR(S)
Sankar Sambasivan, Kimberly A. Steiner, Krishnaswamy K. Rangan, Johan Abadie, Mark Zurbuchen

7. PERFORMING ORGANIZATION NAME(S) AND ADDRESS(ES)

Applied Thin Films, Inc.
1801 Maple Ave. Suite 5316
Evanston, IL 60201

8. PERFORMING ORGANIZATION REPORT NUMBER

9. SPONSORING / MONITORING AGENCY NAME(S) AND ADDRESS(ES)

USAF, AFMC
Air Force Office of Scientific Research
801 N. Randolph St. Room 732
Arlington, VA 22203-1977

NA

10. SPONSORING / MONITORING AGENCY REPORT NUMBER

20040910 059

11. SUPPLEMENTARY NOTES

12a. DISTRIBUTION / AVAILABILITY STATEMENT
Approved for public release; distribution is unlimited

12b. DISTRIBUTION CODE

13. ABSTRACT ***(Maximum 200 Words)***

Non-crystalline materials can be synthesized using a variety of techniques such as thermal evaporation, sputtering, glow-discharge decomposition, chemical vapor deposition, melting and quenching and from polymeric precursor solutions. Among these, solution based synthesis of amorphous oxide materials are well known in the literature. This process is advantageous over other processes because glasses can be formed at lower temperatures by atomic or molecular level mixing of the components in solution. In oxide systems, the molecular design approach has been so far limited to synthesis of crystalline materials. Principals of Applied Thin Films, Inc (ATFI) have discovered new solution derived non-crystalline oxide materials which can resist crystallization up to temperatures as high as 1400 °C, wherein the precursor species are molecularly designed. Under three years AFOSR program ATFI has carried out investigation on this new class of high temperature amorphous materials in order to further understand the precursor chemistry, pyrolysis process and basis of high temperature metastability of the solid product. Research work is also performed in developing technological applications based on the fundamental studies on the properties.

14. SUBJECT TERMS	15. NUMBER OF PAGES
	47
	16. PRICE CODE

17. SECURITY CLASSIFICATION OF REPORT	18. SECURITY CLASSIFICATION OF THIS PAGE	19. SECURITY CLASSIFICATION OF ABSTRACT	20. LIMITATION OF ABSTRACT
Unclassified	Unclassified	Unclassified	UL

APPLIED THIN FILMS, INC.

NEW CLASS OF HIGH TEMPERATURE
PSEUDO-AMORPHOUS OXIDE MATERIALS

Final Report

January 1, 2001- December 31, 2003

Dr. Sankar Sambasivan
(Principal Investigator)

Kimberly Steiner
Dr. Krishnaswamy K. Rangan
Johan Abadie
Dr. Mark Zurbuchen

Applied Thin Films, Inc.
1801 Maple Ave. Evanston, IL 60201

Contract Number: F49620-01-C-0014

TABLE OF CONTENTS

EXECUTIVE SUMMARY

Introduction

Non-crystalline materials can be synthesized using a variety of techniques such as thermal evaporation, sputtering, glow-discharge decomposition, chemical vapor deposition, melting and quenching and from polymeric precursor solutions. Among these, solution based synthesis of amorphous oxide materials are well known in the literature. This process is advantageous over other processes because glasses can be formed at lower temperatures by atomic or molecular level mixing of the multicomponents in solution. In oxidic systems, the molecular design approach has been so far limited to synthesis of crystalline materials. Principals of Applied Thin Films, Inc (ATFI) have discovered new solution derived non-crystalline oxide materials, which can resist crystallization up to temperatures as high as 1400 °C, wherein the precursor species are molecularly designed. Under three years AFOSR program ATFI has carried out investigation on this new class of high temperature amorphous materials in order to further understand the precursor chemistry, pyrolysis process and basis of high temperature metastability of solid product. Research work is also performed in developing technological applications based on the fundamental studies on the properties.

Summary of Fundamental Studies

The new materials investigated under this project are based on aluminum phosphate composition and formed from a clear and homogeneous precursor solution in a variety of physical forms such as bulk powders, fibers, thin films and coatings. Fundamental studies performed under this project were to deduce the structure and chemical characteristics of the precursor solution and the high temperature solid products derived from these precursors. These studies were focused on investigating a) the characteristics of precursor solution, b) the evolution from precursor to pyrolyzed product and c) unique features that contribute to the extended metastability of high temperature product.

The precursor solution is composed of an alcoholic solution of P_2O_5 and $Al(NO_3)_3 \cdot 9H_2O$ in specific molar ratios, which yields a pyrolyzed product of "glassy" $Al_{1+x}PO_{4+3x/2}$, where x represents excess aluminum content over the stoichiometric $AlPO_4$ in the precursor formulation.

Solid products derived from this precursor solution by pyrolysis are black in color in contrast to the conventional colorless aluminum phosphates (hence the name 'Cerablak^{TM}'). Further investigation on the pyrolyzed product using Transmission Electron microscopy and Raman spectroscopy showed the presence of nano-sized carbon embedded in the amorphous aluminophosphate matrix. The amorphous material is metastable resisting crystallization even up to 1400 °C for several hours. The studies under this project showed that this material is not only metastable at higher temperatures but their synthesis requires the presence of molecular species with specific bonding characters in the precursor solution. ^{31}P and ^{27}Al liquid Nuclear Magnetic Resonance (NMR) spectroscopic techniques were used to determine the types of complexes present in the precursor solution. Two essential requirements to obtain high temperature metastable materials are (a) $(OR)_xP{=}O$ and (b) Al-O-Al. These characteristics are deduced based on combined data of several characterization techniques. In the precursor solution, condensation of the aluminum phosphate complexes forming an extended three dimensional Al-O-P polymer is restricted by sterically hindered P=O groups and hydrolytically stable P–OR groups. This chemistry also restricts the formation of aluminum phosphate complexes with only one or two aluminum atoms directly bonded to OP groups. The resulting low condensation kinetics has increased the shelf-lives of precursor solution to several months as compared to less than 24 h shelf life of currently known sol-gel solutions. This aspect of precursor chemistry essentially eliminated one of the major hurdles in commercial application of sol-gel coatings. Pyrolysis of Cerablak™ precursor solution is followed with FTIR spectroscopy in order to determine the pathway from precursor to high temperature material. The high temperature heated Cerablak™ sample contains Al-O-P groups, but in addition, contains Al-O-Al groups directly bonded to Al-O-P groups. These [P-O-Al-O-Al] linkages can exits in precursor solution or can be formed during heat treatment. We believe the majority of excess aluminum species that are not directly bonded to P-O groups are linked to the aluminum of the ester complex in the precursor solution, although direct evidence is still lacking. Presence of such "interrupting" Al-O-Al groups in a continuous network containing Al-O-P linkages resist the nucleation of both crystalline $AlPO_4$ and Al_2O_3, thus retaining the amorphous character to elevated temperatures. The thermal stability is extended to higher temperatures with increasing amount of excess aluminum in the precursor solution (x= 0 to 3).

The reason for the extended stability of Cerablak™ at elevated temperatures can be attributed to the low oxygen diffusivity of the material. Indirect evidence for the low oxygen diffusivity of the amorphous material is extended by the fact that nano-sized carbon particles are retained in samples heated elevated temperatures up to 1400 °C. Estimated chemical diffusivity values ranged between 1 x 10^{-9} to1 x 10^{-10} cm^2/sec which is extremely low and reduces the rearrangement of atoms by restricting their mobility which required for crystallization to occur.

Summary of Technology Development

Much of the technology development under this project is made on Cerablak™ as thin film on hard substrates such as metal, glass and ceramics. Surface modification of such substrates, via deposition of thin films, has enabled generation of numerous products. Among the commonly-known uses are surface passivation for protection against harsh chemical environments and high temperature exposure, electrical and thermal insulation, wear and abrasion resistance, non-stick, non-wetting, surface planarization, and surface-modified biological systems. While polymer and, more recently, organic-inorganic hybrid films serve adequately for some of the aforementioned applications, thin inorganic films are desired due to their inherent hardness and durability and to serve many high temperature applications. Developing pin-hole free, thin and thermally stable inorganic films using low-cost solution-based stable precursor solutions has been a long-standing challenge for material scientists. Cerablak™ is a unique amorphous inorganic oxide material with desirable thin film properties derived from a clear, shelf-stable, low-cost precursor solution.

Due to its extremely low oxygen diffusivity and the hermetic nature, ultra-thin films are sufficient to provide the necessary protection in many cases. A nominal one micron (or less) thick hermetic film deposited using simple dip-coating or spray or other methods has demonstrated excellent protection against high temperature oxidation and atmospheric corrosion. Film stability under thermal cycling conditions is critically important for many applications and the thin nature of these films will help to minimize the residual thermal stresses such that cracking and spallation is prevented. In addition, these films offer suitable non-stick, non-wetting, and surface planarization characteristics which are critically needed for many industrial, consumer, and military applications. Another important aspect of Cerablak™ coating is on glass

substrates. It helped to impart hydrophobic nature to glass surfaces which can be used in several applications such as windows, etc. Thus, it is the combination of various attributes of this new development that lends to practical use and places it in a special class of materials with broad commercial potential.

Final Assessment

The discovery of this unique class of high-temperature amorphous materials opens up numerous technological opportunities while posing intriguing questions regarding novel molecular-design approaches to creating an entirely new class of materials in other chemical systems, which can exhibit interesting properties. The result of fundamental studies on the new aluminum phosphate composition has shown an interesting correlation between precursor chemistry and the stability of high temperature material. This study has established that new high temperature stable amorphous oxide materials can be prepared by controlling precursor chemistry. This approach can be extended to other materials systems by suitably designing the molecular complexes, which can prevent or form the specific atomic links leading to highly stable amorphous oxides.

LIST OF FIGURES

I. PROJECT INTRODUCTION AND ACKNOWLEDGEMENTS

Solution based synthesis of amorphous oxide materials is well known in the literature. This process is advantageous over conventional melting and quenching of glass because glasses can be formed at lower temperatures by atomic or molecular level mixing of the components in solution [1]. This method also has potential to obtain glasses from reluctant glass-forming systems. However, the thermal stability of the glasses formed by solution-based synthesis is always much lower than those prepared by conventional methods. Recently, it has been shown in the synthesis of Si-B-C-N amorphous materials that the thermal stability of the amorphous non-oxide materials formed can be controlled by molecularly designing the polymer precursors. In oxide systems, the molecular design approach has been so far limited to synthesis of crystalline materials. A new sol-gel method for the synthesis of amorphous aluminum phosphate wherein the precursor species are molecularly designed to yield non-crystalline material, which can resist crystallization up to temperatures as high as 1400 °C was studied under this program. This new approach raises the possibility of discovering new thermally stable amorphous oxides through the control of precursors.

Non-crystalline aluminophosphates can be prepared at low temperatures by a variety of synthetic of routes [2,3,4]. However, all of those amorphous materials crystallize below 1000 °C forming thermodynamically stable cristobalite $AlPO_4$ and α-Al_2O_3. For example, pyrolysis of reaction mixtures containing H_3PO_4 or $POCl_3$ with $Al(NO_3)_3$ gives amorphous aluminophosphates which crystallizes at 800 °C. On the other hand, crystalline $AlPO_4$ can be obtained by a sol-gel reaction between aluminum alkoxide and H_3PO_4 even at 180 °C [5]. We have synthesized amorphous aluminophosphates materials $AlPO_{4+3x/2}$ from a precursor formulation consisting of a mixture of P_2O_5 and $Al(NO_3)_3$ in alcohol. x represents excess aluminum content over the stoichiometric $AlPO_4$ in the precursor formulation. The high-temperature stability this precursor derived material prompted us to investigate the factors responsible for its exceptional thermal stability, and was the impetus for this basic science program. Accordingly, we studied the chemistry of precursor solution and structural evolution of high temperature solid products derived from these solutions.

Acknowledgements

This research was supported by the Air Force office of Scientific Research (AFOSR) under Grant F49620-01-C-0014.

.

The authors thank the following individuals for helpful discussions and contributions: Richard W. Goettler (Mcdermott Technology, Inc.), Alexandra Navrotsky (UC-Davis), George A. Wolf (Arizona State University), and David A. Richardson (Consultant).

Project Participants

Name	Position	Role In Project
Dr. Sankar Sambasivan	President & CEO	Principal Investigator
Kimberly Steiner	Research Scientist	Precursor Chemistry, XRD
Johan Abadie	Research Scientist	Precursor Chemistry, Coating Development
Dr. Krishnaswamy K. Rangan	Research Scientist	Precursor Chemistry, Analysis (XRD, NMR, FTIR)
Dr. Mark Zurbuchen	Research Scientist	TEM
Francis Chapman	Research Engineer	SEM
Stephanie Portle	Co-operative Education Student	Precursor Chemistry, Coating Development
Brian Fisher	Co-operative Education Student	Precursor Chemistry
John Joo	Co-operative Education Student	Precursor Chemistry
Benjamin Mangrich	Co-operative Education Student	Precursor Chemistry

II. FUNDAMENTAL STUDIES ON STRUCTURE AND PROPERTIES OF AMORPHOUS ALUMINUM PHOSPHATE

A. Precursor Chemistry

The precursor solutions are prepared according to a patented method, composing of an alcoholic solution of P_2O_5 and $Al(NO_3)_3 \cdot 9H_2O$ in specific molar ratios [6]. The alcohols such as methanol, ethanol, and butanol can be used in the synthesis. The compositions varied from Al/P ratio of 1 to 10. Reaction between P_2O_5 and alcohol, ROH where, $R = C_nH_{2n+1}$ (n = 1, 2, or 4), results in corresponding phosphate esters according to the stoichiometry given by the following equation:

$$P_2O_5 + 3\ ROH \longrightarrow OP(OR)(OH)_2 + OP(OR)_2(OH) \qquad (1)$$

A small amount of phosphoric acid and trialkyl phosphates are also formed during this reaction [7]. Liquid ^{31}P nuclear magnetic resonance spectra (NMR) were recorded on a Varian-Mercury 400 spectrometer using frequency 202.281MHz with a sample spin rate 20 Hz. The external standard used is 85% H_3PO_4. The ^{31}P NMR spectrum of the solution is given in Figure 1 and shows two strong peaks at +0.17 ppm and -0.07 ppm corresponding to mono and dialkyl phosphate esters respectively.

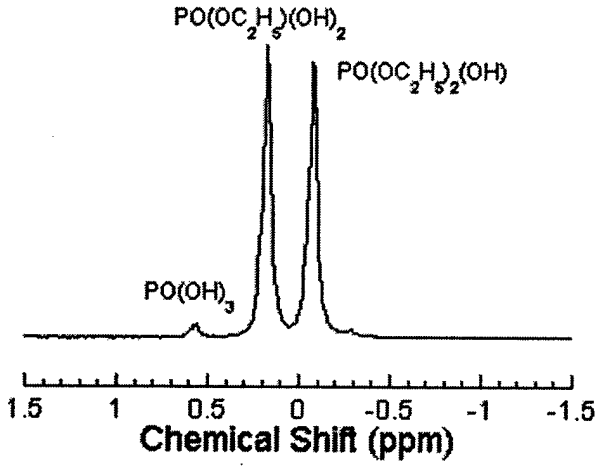

Figure 1. ^{31}P NMR spectrum of P_2O_5 in ethanol

On adding Al^{3+} solution to this phosphate esters mixture, a clear solution resulted without precipitation or gel formation. The precursor solution can be prepared with a range of Al:P ratio compositions of x = 0 - 9, where *x* represents excess aluminum molar content over the

phosphorus. For example, for a stoichiometric composition of Al:P of 1:1, x will be 0; for Al:P of 2:1, x will be 1, and so on. The solutions remain clear for several months. The ^{31}P NMR spectrum of the aluminum phosphate mixture, x = 1 (Figure 2) shows predominantly two strong resonance peaks near -6 ppm and -12 ppm.

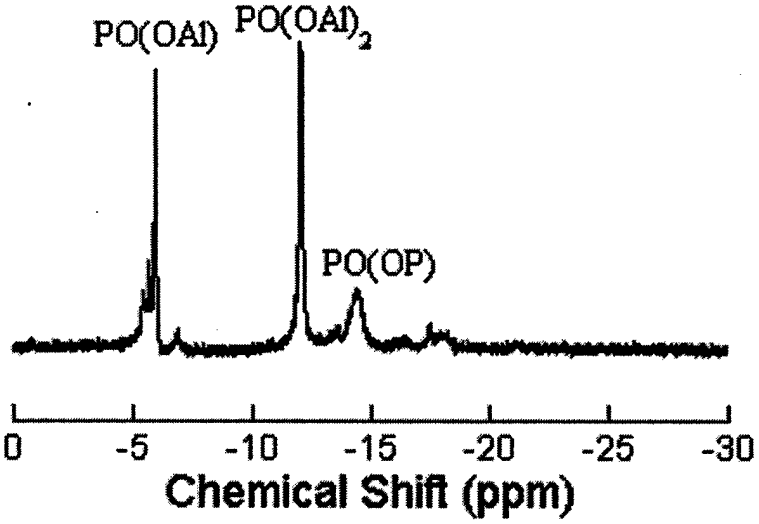

Figure 2. ^{31}P NMR spectrum of mixture of P_2O_5 and aluminum nitrate (x = 1) in ethanol

Based on their chemical shift values these peaks can be attributed to phosphate esters bonded to one or two Al atoms respectively. These aluminophosphate complexes can be represented schematically as (1) and (2) respectively [8], with a mixture of alcohol and water molecules coordinated to aluminum.

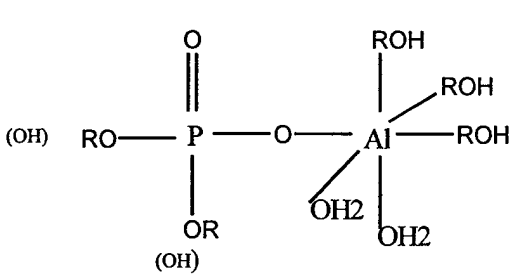

(1)

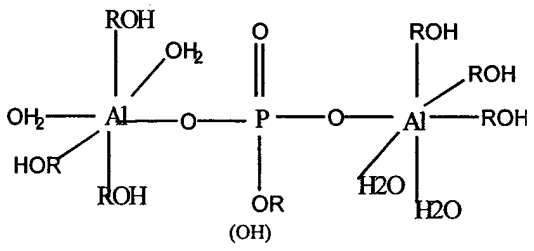

(2)

The ratio of the amount of these two aluminophosphate species seems to depend on the size of the alkyl groups. For example, in methanol $P(OAl)_2$ clusters are predominant and in butanol P(OAl) observed as major species. This is probably due to the steric effects of alkyl groups of the phosphate esters which hinder the attack on phosphorous by (Al-O) groups.

The broad peak centered at -14ppm could be assigned to PO(OP) type complexes. This assignment is indirectly supported by the following observation. The intensity of -14ppm peak decreases with the increase in aluminum content (from Al/P ratio 1 to 4) (Figure 3).

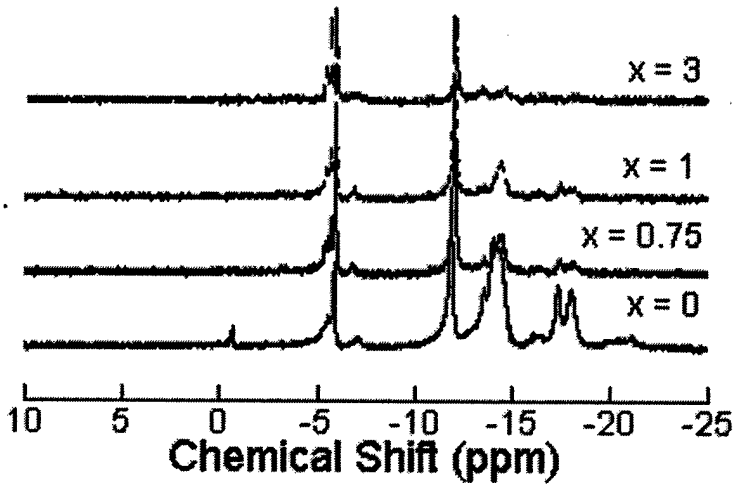

Figure 3 ^{31}P NMR spectrum of Cerablak precursor solutions as a function of composition in ethanol.

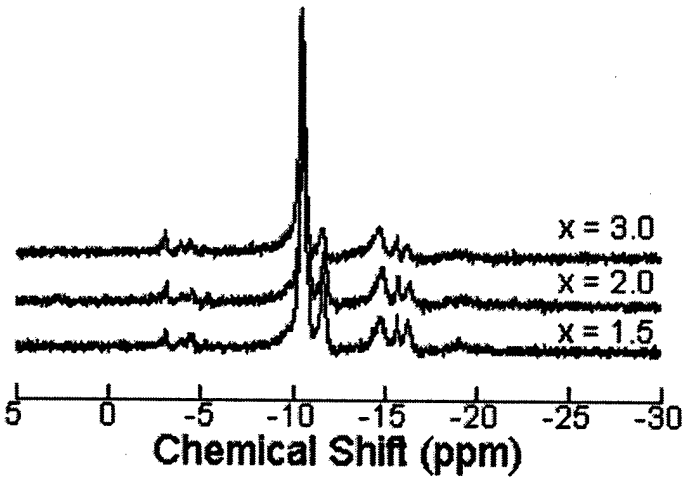

Figure 4 ^{31}P NMR spectrum of Cerablak precursor solutions as a function of composition in methanol

Similar trend is also observed in the methanol based precursor solutions. ^{31}P liquid NMR spectra of precursor solution with Al/P composition x – 1.5 to 3 are plotted in Figure 4. In this case P(OP) resonance occurs at -11.6 ppm. The chemical shift values observed are different from ethanol based precursor solutions, probably because of the solvent effects and the changes in the secondary and higher coordination spheres. As discussed above $PO(OAl)_2$ type species are predominantly present in the methanol based solution.

Further condensation of these ester complexes **(1)** and **(2)** can lead to extended polymeric structure in solution. However, we observe only limited polymerization occurring in precursor solution. It is interesting to note that the viscosity of the solution remains almost constant after several hours. Aluminophosphate complexes terminated with alkyl groups can prevent the extensive condensation limiting cluster size of the polymers. The small-size of polymers in turn results in clear solutions which are stable for years without gelation or precipitation. In contrast, silica based precursor solutions normally result in larger sized sol particles up on aging or refluxing and have limited storage stability of less than 24 h before gelation occur. Viscosity of silica based solutions also increase on storage and modify the coating properties. This is one of the major hurdles in using sol-gel coatings in industry that is removed in the case of Cerablak™ precursor solutions.

Formation of either of the two species **(1)** and **(2)** shown above establishes the presence of P-O-Al linkages in the precursor solution. ^{27}Al liquid NMR spectroscopic analysis of Cerablak™ precursors was performed in order to further understand the Aluminum coordination sphere. Presence of Al-O-Al type bonding can be deduced by ^{27}Al NMR spectroscopic data. Figure 5 shows the presence of broad resonance peak centered at -1 ppm corresponding to Al(OP) groups and a sharp peak due to $Al(OP)_2$ groups. As -OP groups are substituted by –OAl groups in the first coordination sphere of Al, the chemical shift values moved to more positive values. A broad peak centered at +8 ppm, thus can be assigned to Al(OAl) groups. It is interesting to note that the amount of monomeric uncoordinated-aluminum is <1.5%. Al-O-Al groups can be either linked

into the ester complex to form a cluster representing [(O)P-O-Al-O-Al-] types freely exists in the precursor solutions. We believe the Al-O-Al linkage is part of the ester complex; the primary reason being that Al-O-Al linkages do not form in pure aluminum salt alcoholic or aqueous solutions [9]. Indirect evidence of their association with the ester group is also observed by varying the Al/P stoichiometry in the formulations. For $x = 0$, formation of complexes with Al/P >1 would result in excess phosphate esters that are not complexed with aluminum. Correspondingly, for $x = 0$, the ^{31}P NMR spectra show a resonance peak near -14 ppm, related to P(OP) group [10], and the peak intensity decreases with increasing aluminum content. These results support the formation of multi-cation clusters with Al/P ratio ≥ 2 in solution leading to [O=P-O-Al-O-Al] cluster formation.

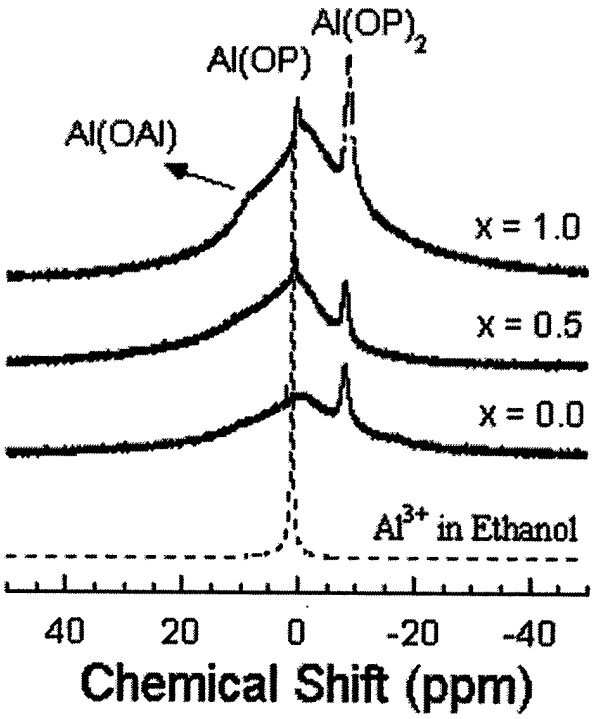

Figure 5. ^{27}Al liquid NMR spectra of Cerablak precursor solution as a function of composition. Spectrum for ethanolic solution of aluminum nitrate is also provided for comparison.

It is interesting to note that the amount of monomeric uncoordinated-aluminum is <1.5%. Al-O-Al groups can be either linked into the ester complex to form a cluster representing [(O)P-O-Al-O-Al-] types or freely exist in the precursor solutions. We believe the Al-O-Al linkage is part of the ester complex; the primary reason being that Al-O-Al linkages do not form in pure aluminum salt alcoholic or aqueous solutions [11]. Indirect evidence of their association with the ester group is also observed by varying the Al/P stoichiometry in the formulations. For $x = 0$, formation of complexes with Al/P >1 would result in excess phosphate esters that are not complexed with aluminum. Correspondingly, for $x = 0$, the ^{31}P NMR spectra show a resonance peak near -14 ppm, related to P(OP) group [12], and the peak intensity decreases with increasing aluminum content. These results support the formation of multi-cation clusters with Al/P ratio ≥ 2 in solution leading to [O=P-O-Al-O-Al] cluster formation.

B. Pyrolysis of Precursor Solution

Cerablak™ precursor solution on drying forms a colorless gel powder which on pyrolysis at elevated temperatures results in 'jet-black' powders, unlike conventional aluminum phosphate materials, which are colorless. Thermogravimetric analysis of dried powder showed a weight loss of 50 -30% depending on the Al/P composition (Figure 6). Solvents and organic groups are removed below 400 °C. On further heating the sample up to 1300 °C there is no appreciable weight loss observed.

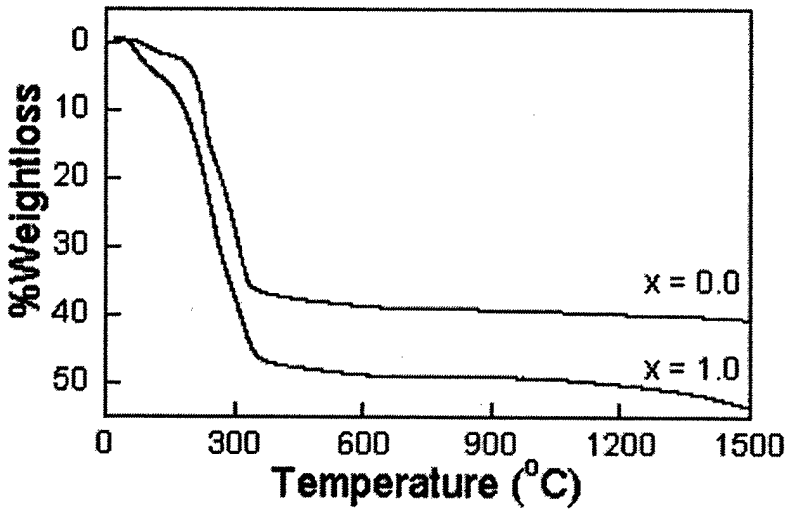

Figure 6 TGA curves of Cerablak™ gel powder with compostions x =0 and x=1.

In order to investigate the thermal events leading to pyrolyzed solid product we have recorded Differential Thermal Analysis data of the dried powder (Figure 7). A broad weak exotherm centered at 300 °C. This corresponds to the oxidation of hydrocarbons associated with the ester groups. The broad nature of the peak suggests that the organic molecules are trapped in the inorganic matrix gel. This is in contrast to the sharp exothermic peaks generally observed with decomposition of organics. For example, precursor solution from an unrefluxed solution of triethyl phosphate and aluminum nitrate showed sharp exothermic peaks due to decomposition of organics which can freely leave the inorganic matrix. A very weak exotherm shoulder is visible in the DTA near 1050 °C, which could correspond to the nucleation of nanocrystals. Most interesting factor is that there is no strong exothermal peak corresponding to the crystallization of the aluminum phosphate or alumina is not observed in the DTA curve showing the amorphous metastability of the Cerablak™ material. In comparison, sharp exothermic peaks near 1000 °C are reported for aluminum phosphate materials precipitated from aluminum nitrate and phosphoric acid. The base line of the DTA curve is drifted from the center up to 1100 °C. This could be due to the formation of nanosized carbon from the organics trapped in aluminum phosphate matrix and its oxidation at elevated temperatures.

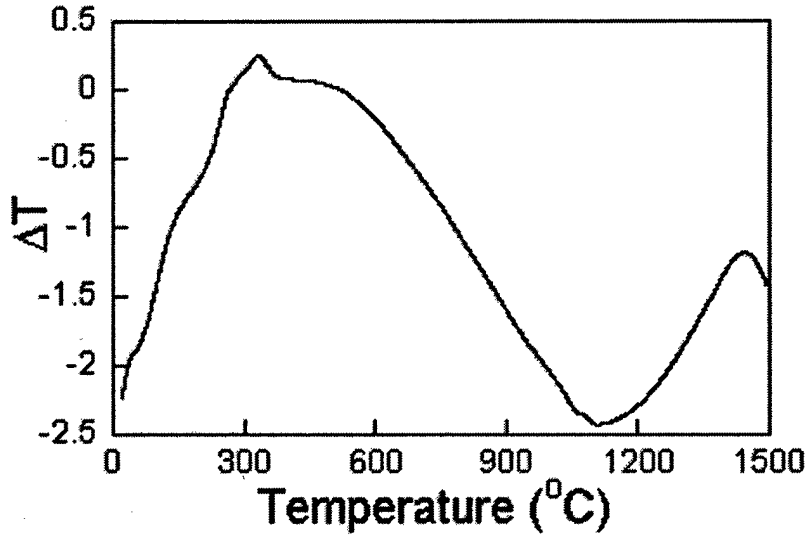

Figure 7 DTA plot of Cerablak of composition x = 1

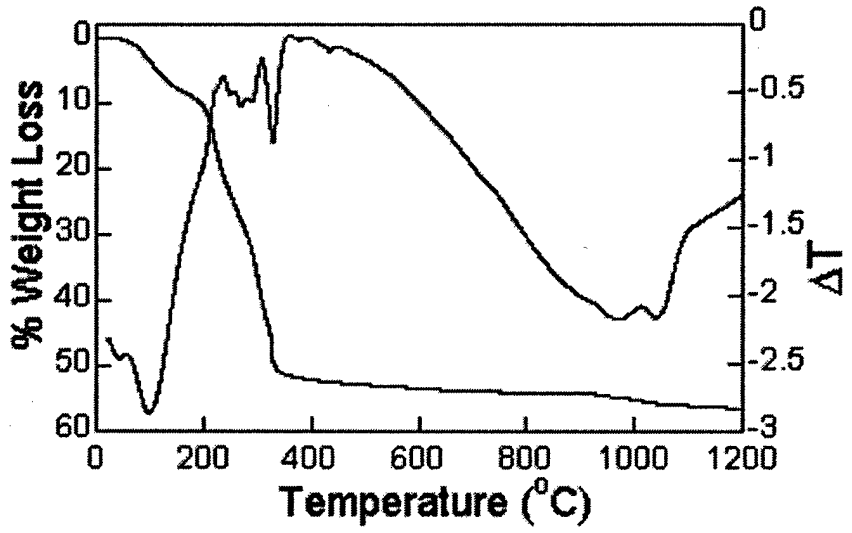

Figure 8. TGA and DTA plot of dried powder derived from unrefluxed triethyl phosphate and aluminum nitrate.

C. Characterization of Pyrolyzed Solid Products

The solid product obtained from pyrolysis of the precursor solution is heat treated at a range of temperatures in order to study its thermal stability. Figure 9 shows the photographs of the powder sample heat treated from 1000 °C to 1600 °C for a range of duration.

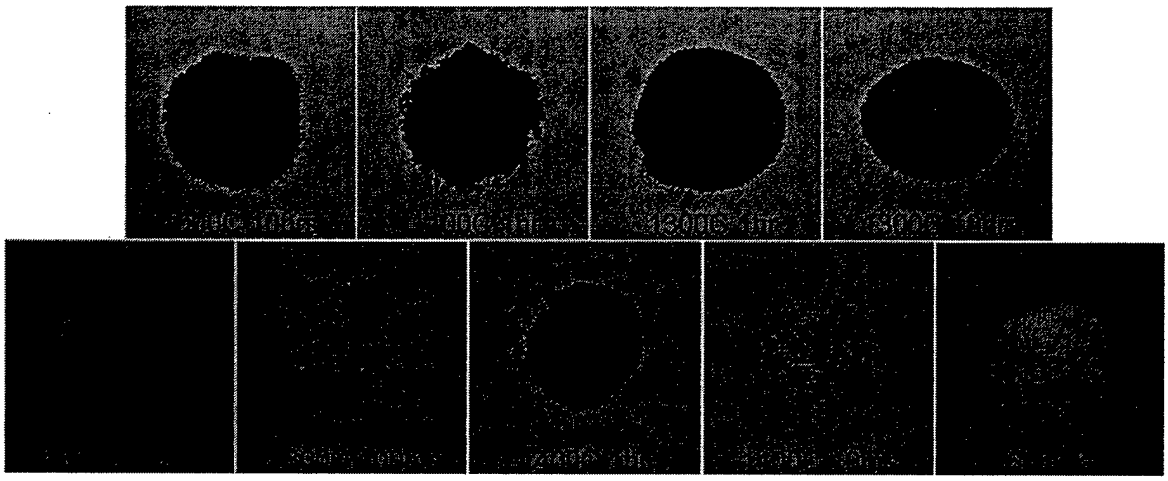

Figure 9 Photographs showing Cerablak powders heated treated up to various high temperatures

Characterization of the samples were performed using a variety of techniques including X-ray diffraction (XRD), Transmission Electron Microscopy (TEM), FTIR, Raman and solid state NMR spectroscopy.

a. Powder X-ray Diffraction Analysis

Non-crystalline nature of Cerablak™ materials were followed by powder X-ray diffraction (XRD) analysis. Powder XRD patterns were acquired on a Scintag (40 kV, 40 mA) using Cu Kα radiation source. The scan rates were between 0.10 and 0.15 deg/min and a step size of 0.01 deg. Figure 10 shows the evolution of structure of Cerablak™ material with x = 1 as a function of temperature treatment. Powder XRD patterns of samples heated up to 900 °C show only broad humps, indicating the completely amorphous nature of the material. On heating further, broad peaks appear at 21.7 and 36 deg.

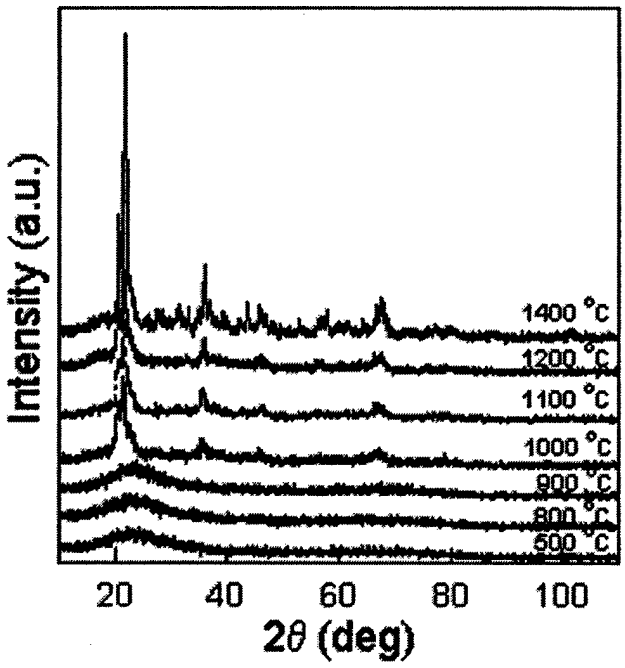

Figure 10 Powder XRD patterns showing the evolution of structure of Cerablak as function of temperature (x=1).

Powder XRD patterns of Cerablak™ bear a striking similarity to those of certain silicate opalline minerals [13].This comparison reveals interesting insights on the nature of nanocomposites observed with aluminophosphates. Opal minerals are silica, arising from a low temperature hydrothermal diagenetic process [14] and contain nanocrystallites of tridymite and cristobalite of the size from 12 to 32 nm encapsulated in the amorphous silica matrix. In Figure 11, we compare the XRD patterns of Opal-CT with that of the Cerablak™. The patterns are almost identical suggesting the Cerablak™ represents a structural analog of silicate opals.

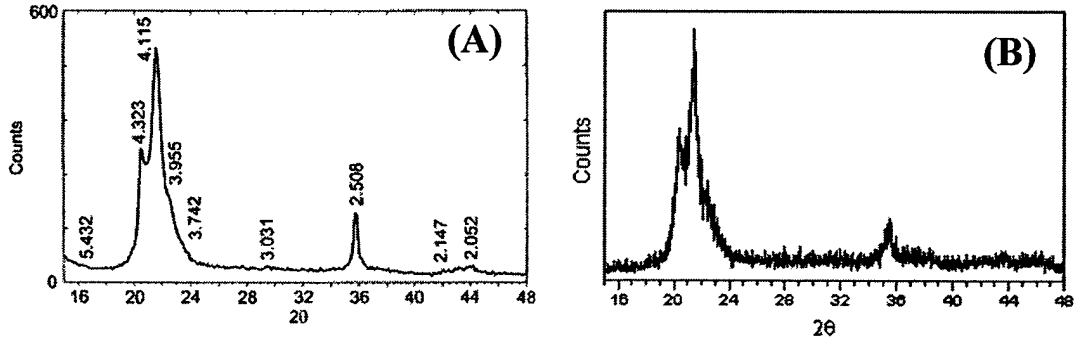

Figure 11. Powder XRD patterns of (A) Opal-CT (from Ref. 13) and (B) Cerablak™ (x = 0.75) calcined at 1100 °C, 1 h.

Both silicate opals and Cerablak™, show broad features around 21° (2θ) and a weak peak around 35°. The position and width of the 21° peak is a consequence of the combination of two unresolved peaks, α-cristobalite (101) and α-tridymite ($40\bar{4}$), as well as non-Bragg scattering phenomena arising from amorphous matrix.

Local structure using PDF analysis

In order to probe the local structure of the pyrolyzed amorphous product, we analyzed the X-ray diffuse scattering with the atom pair distribution function technique (PDF). Amorphous materials do not show sharp Bragg peaks in the Powder XRD pattern because of lack of long range structural order. However, short range order result in diffuse scattering and appear as broad humps in the XRD pattern (Figure 12A).

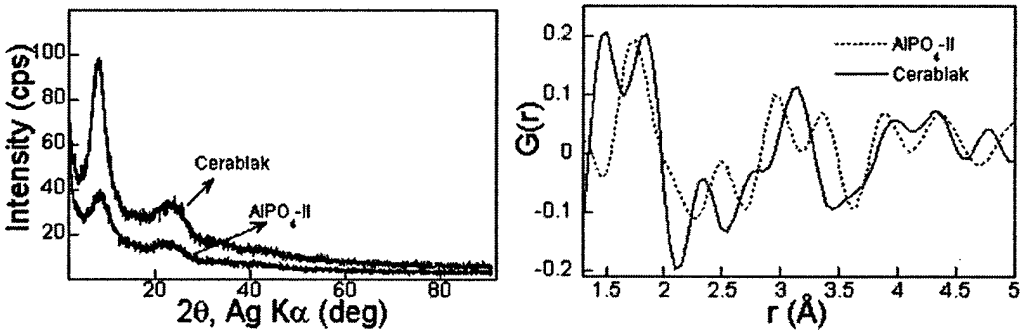

(A) (B)

Figure 12. (A) Powder XRD pattern of Cerablak™ pyrolyzed at 800 °C and aluminophosphate ($AlPO_4$-II) prepared at 800 °C from aluminum nitrate and phosphoric acid. (B) Reduced pair distribution function, G(r) of Cerablak™ and $AlPO_4$-II plotted against distance *r*.

This diffuse scattering data contains a great deal of information, about local structure and bonding. When the XRD data are Fourier transformed into real-space coordinates, we obtain the atomic pair distribution function (PDF). This is simply another representation of the powder diffraction data; however, it can often be revealing and helpful to study the data in real-space. The XRD data for the PDF determination were collected using Ag K_α radiation. The data were corrected for background, absorption, polarization, Compton, and multiple scattering and normalized by the incident flux, the number of scatterers, and the average atomic form factor of

the sample to obtain the normalized total scattering function S(Q) ($Q=4\pi \sin\theta/\lambda$ where 2θ is the scattering angle and λ wavelength of radiation).

The reduced radial distribution function, or PDF, G(r) is obtained from S(Q) through a Fourier transform. The function G(r) represents the radial density distribution showing peaks at distances, r, which separate pairs of atoms in the solid (Figure 12B). For example, the strong peak occurs at r = 1.84 Å corresponding to the Al—O nearest neighbor peak in these materials. It is a measure of the short-range atomic order in the solid [15]. In Table 1, we list the prominent peak values for (a) Cerablak™, (b) $AlPO_4$-II, a type of aluminophosphate prepared from aluminum nitrate and phosphoric acid in an aqueous medium, and (c) literature data [16] for an amorphous $AlPO_4$ material ($AlPO_4$-III), along with the possible atom pair assignments.

Table 1. PDF data of aluminophosphates derived from different synthetic routes

Cerablak™ (Å)	$AlPO_4$-II (Å)	AlPO4-III (From Ref. 3) (Å)	Assignment of Atom Pair Distances
1.48	-	-	C-C
1.84	1.74	1.6	P-O/Al-O
2.34		-	O-O (PO_4)
	2.5	2.6	O-O (PO_4 or AlO_4)
2.79		-	O-O (AlO_4)
3.14	2.95	3.1	Al-P
	3.35		Al-Al
3.94	3.88		Al-O(2^{nd})/ P-O(2^{nd})
4.31	4.35	4.2	Al-O(2^{nd})/ P-O(2^{nd})

All three materials show characteristically different atom-to-atom distances which is typical of amorphous structures with varying degrees of bonding and coordination. The peaks corresponding to Cerablak™ appear to vary to a greater degree when compared with other two materials. The presence of peak corresponding to 1.48 Å for the Cerablak™ is absent in other

two materials. This peak value compares well with C-C bond length found in carbon materials, thus indicating the presence of carbon in Cerablak™ which has also been confirmed by other methods. The average bond length represented by peak centered at 1.84 Å for Cerablak™ is higher than expected average bond length value of 1.72 Å. Instead of one peak centered at 2.6 Å expected for O-O distance, PDF of Cerablak™ shows two peaks corresponding to 2.34 Å and 2.79 Å. These two distances could correspond to O-O distances from O-P-O and O-Al-O groups. Peaks at 3.14 Å and 3.94 Å can be interpreted as Al-P (Al-Al) and Al - O2nd atom pair distances. No significant atom- atom correlation peaks are observed at distances higher than 5 Å indicating the absence of long range order in Cerablak™ . The PDF study provides critical information necessary to define the network structure of Cerablak™ and the associated low oxygen diffusivity observed. Other complimentary analysis using spectroscopic and diffraction methods will be required to complete the structural characterization.

b. Transmission Electron Microscopy

Powder samples were prepared for TEM examination by crushing in methanol to obtain fresh, thin regions for examination. A Hitachi HF-2000 cold field-emission TEM, operated at 200 kV, was used for microscopy. Bright field images were collected slightly under-focus to enhance edges and interfaces, to aid in discerning nano-inclusion boundaries. Because the microscope does not have a selected area (SA) aperture, steps were taken to acquire pseudo-SA electron diffraction (ED) patterns with illumination that was as close to parallel as possible. This was achieved by using the smallest condenser aperture (50 μm) and expanding the beam to the largest possible size for the area of interest. This also significantly decreased sample irradiation. Care was taken to find "fresh" areas for each set of data taken, so that potential issues of sample amorphization could be avoided. Long-time exposure tests indicated no discernable sample damage from such a beam.

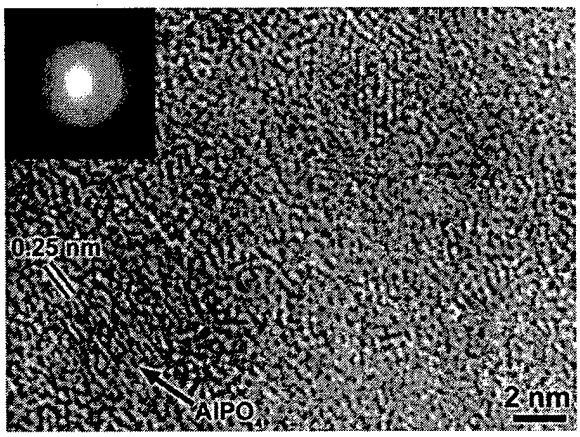

Figure 13. TEM bright field image showing small $AlPO_4$ crystallite in an amorphous matrix.

Based on XRD analysis, it is apparent that nanocrystals in these powder materials begin to nucleate around 1100 °C. TEM analysis supports this and further provides evidence that these nanocrystals are completely isolated and encapsulated in the amorphous matrix (Figure 13). With increasing temperature and time of annealing, the nanocrystals grow and typically range in sizes of 5-100 nm. Due to the presence of the stable amorphous matrix, their growth is limited even at 1400 °C. Occasional presence of large crystals (>100 nm) are observable at very high temperatures (Figure 14). Energy Dispersive Spectroscopy (EDS) performed on these materials show the presence of varying amounts of Al, P and O.

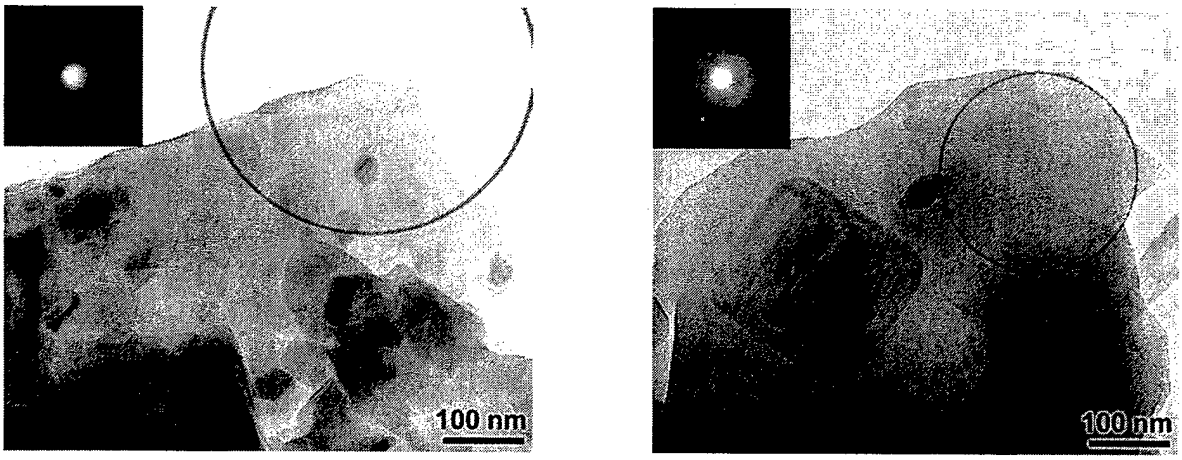

(A) (B)

Figure 14. Representative bright field TEM images of the Cerablak™ after annealing at (A) 1200 °C for 420 h and (B) 1400 °C for 10 h. Electron diffraction pattern in the insets were collected from the circled regions. The halo in the diffraction patterns clearly shows the material to be amorphous, and also shows a few diffraction spots from the nanocrystals ($AlPO_4$) encapsulated in the amorphous matrix.

As described earlier, the decomposition behavior of thin films is quite different and leads to the formation of completely amorphous materials even after annealing to elevated temperatures for prolonged periods of time (Figure 15).

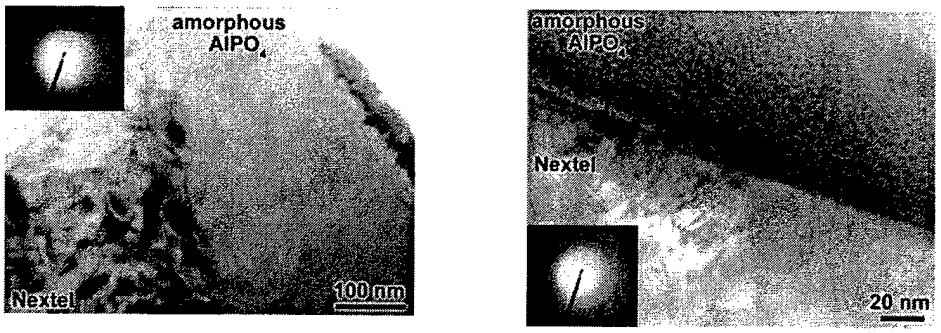

(A) (B)

Figure 15. TEM micrographs and electron diffraction patterns of aluminophosphate coated fiber (Nextel™ 720) annealed at (A) 1200 °C, 1 h and (B) 1200 °C for 100 h. The insets are electron diffraction patterns of the aluminophosphate coated regions indicating the completely amorphous nature of the film.

While no corundum peaks are seen in the XRD patterns of powders (Figure 10) heated to 1100 °C. TEM evidence indicates the presence of nanocrystals of corundum. Figure 16 shows the d-spacing of rings which appear in the electron diffraction pattern, along with the d-spacings

from corundum, tridymite and cristobalite $AlPO_4$. Some of the rings apparent in the Cerablak™ diffraction pattern appear to coincide with that of corundum, rather than $AlPO_4$, indicating the presence of nanocrystals of corundum. Diffraction rings with a d-spacing of less than 2Å are likely to be due to corundum.

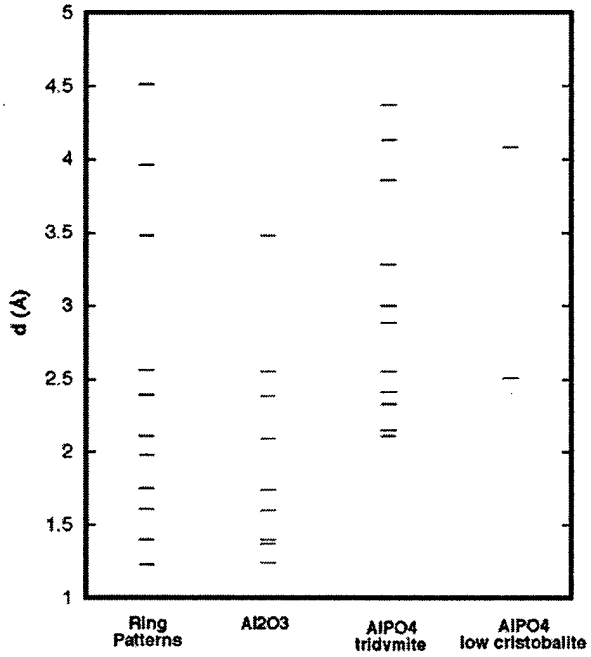

Figure 16. D-spacing of Cerablak™ diffraction pattern along with d-spacings of crystalline alumina and aluminum phosphate.

c. Fourier Transform Infrared Spectroscopy

FTIR technique is employed in order to understand more about the pyrolysis of precursor solution and the bonding characteristics of amorphous product. Figure 17 shows the FTIR spectra of Cerablak™ samples of composition x = 0.75 as a function of temperature. FTIR spectrum of gel powder obtained by drying precursor solution at 150 °C showed a sharp peak at 1382 cm^{-1}, which can be assigned to P=O stretching and absorption peaks corresponding to P-OC_2H_5 ester groups appear at 1716,1483, 1327 and 1038 cm^{-1} frequencies. These peaks are not observed on further heating to 250 °C

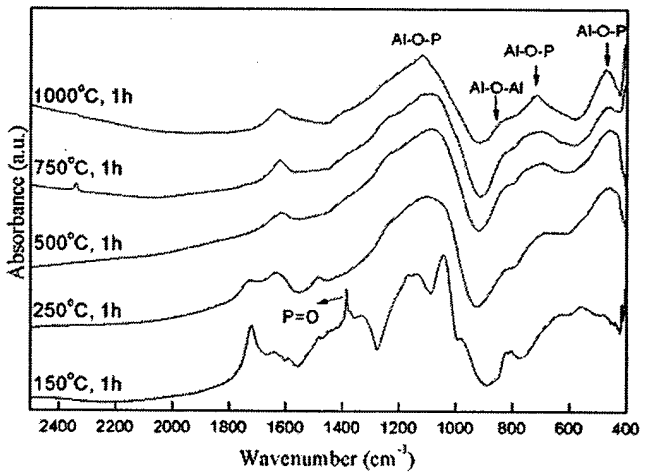

Figure 17 FTIR spectra of Cerablak™ as a function of temperature

Figure 18 shows the FTIR spectra of Cerablak™ materials heated at 1100 °C for 1 h, as a function of composition (Al/P ratio). PO_4 asymmetric stretching frequencies of Cerablak™ materials observed at 1100-1200 cm^{-1} are similar to those of crystalline polymorphs of $AlPO_4$. However, the bands are broad due to the amorphous nature of material. PO_4 bending bands of Cerablak™ appear at frequencies between that of cristobalite and tridymite forms. In addition to PO_4 and P-O-(Al) bands there is a shoulder appear near 830 cm^{-1} for Cerablak™ (x=0.75) material which has excess aluminum than the stoichiometric $AlPO_4$ composition. The intensity of this band increases with increase in aluminum content and therefore can be assigned to Al-O-Al stretching.

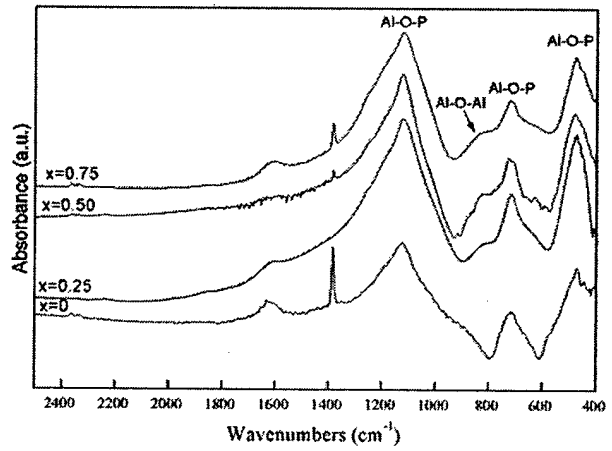

Figure 18. FTIR spectra of Cerablak™ as a function of Al/P ratio

Table 2 Assignments of bands for various forms of aluminum phosphate (position of bands in cm^{-1})

Cristobalite	Tridymite	Cerablak (x = 0)	Cerablak (x=0.75)	Band Assignment
1231 (sh)	1246 (sh)			
1126 (s)	1134 (s)	1124	1121	PO_4 Asymmetric Stretching
-	-	913	-	P-O-(P)
-	-	-	830	Al-O-(Al)
735				
	727 (w)	714	717	Al-O-(P)
714				
623				
565				
500				
465	488	473	476	PO_4 Bending

d. Solid State NMR Spectroscopy

NMR spectroscopy is an excellent tool to analyze atomic coordination, and it provides important clues regarding the coordination of aluminum that may be relevant to determining the nature of bonding in the amorphous network. Solid-state ^{27}Al NMR experiments were performed on a 360-1 spectrometer (Spectral Data Services, IL) operated at 94.6 MHz. All spectra were referenced to an external standard of $[Al(H_2O)_6]^{3+}$ in dilute aqueous aluminum nitrate (Figure 19A). The resonance position is reported between 40 and 70 ppm for tetrahedral aluminum Al(IV) , around 25-30 ppm for the pentacoordinated aluminum Al(V) , and at 0-12 ppm for the octahedrally coordinated Al(VI). In Figure 19 it can be seen that tetrahedral and octahedral coordinated aluminum are observed. Deconvolution of the NMR spectra revealed several features in the tetrahedral and octahedral regions that correspond to the amorphous content (Figure 19 C & D). These features are apparent even for powder samples annealed to 1400 °C for 36 h, suggesting presence of significant amorphous content. Although some of the peaks centered in the range of -5 to +15 ppm are related to crystalline alumina phases [17], we believe bulk of the aluminum coordinations in that region correspond to the amorphous content. Several other points are noteworthy from Figure 19 C; a) the octahedral peak intensity for $x = 0$, has

virtually disappeared after prolonged high temperature treatments where the corresponding XRD patterns show highly crystalline content, b) the integrated intensity of the broad octahedral peak in $x = 0.75$ samples is a significant fraction of all the aluminum and suggests the material to be substantially amorphous as determined by the XRD and TEM analysis, and c) based on the chemical shifts observed at +7 ppm and +62 ppm, presence of γ-alumina can be inferred in samples with excess aluminum annealed to 1100 °C, 163 h whereas, for the 1400 °C annealed samples, a broad peak near +9 ppm is observed which is partly due to α-alumina based on the evidence from XRD. The reported resonance for α-alumina ranges from +11.3 to +12 ppm [16]. ^{31}P NMR spectrum of Cerablak™, calcined at 1100 °C, is given in Figure 19 E, showing the symmetric environment for phosphorous similar to that observed in crystalline $AlPO_4$.

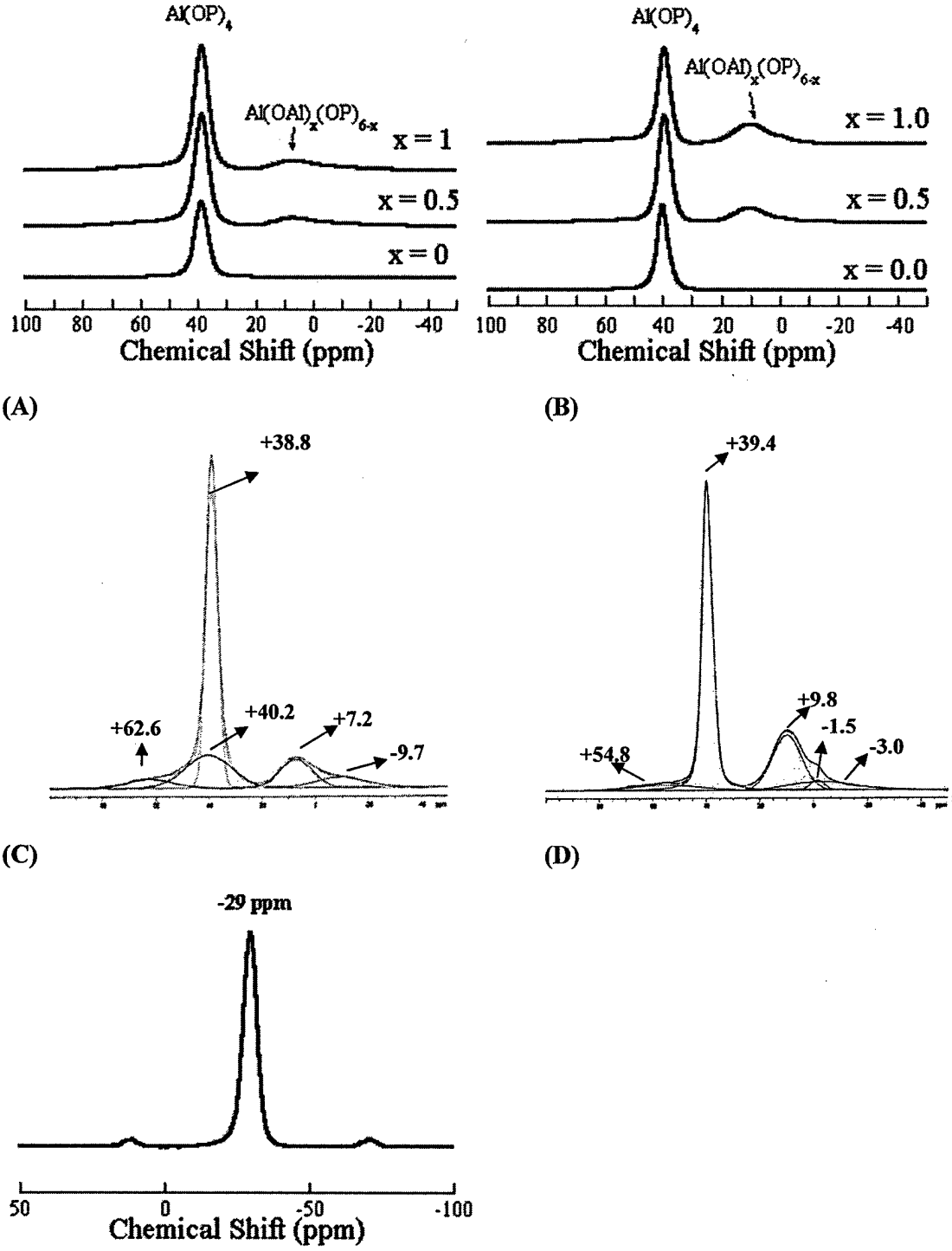

Figure 19. Solid state ^{27}Al NMR spectra of Cerablak™ heated at (A) 1100 °C and (B) 1400 °C as a function of Al/P ratio. Solid state ^{27}Al NMR spectra of Cerablak™ (x = 1) heated at (C) 1100 °C and (D)1400 °C with deconvolution of resonance peaks showing aluminum existing in various coordination environments and (E) Solid state ^{31}P NMR spectrum of Cerablak™ calcined at 1100 °C.

e. Raman Spectroscopy

As described earlier, powders obtained from pyrolysis contained 4-8wt % of elemental carbon after annealing for 1 h at 1100 °C. While carbon loss was seen during subsequent heat treatments at higher temperatures, some carbon was still present even after 1400 °C annealing in air. The color also serves as an indirect indicator of (a) the amorphous nature of the material as carbon inclusions are completely encapsulated in the amorphous matrix, and (b) low oxygen diffusivity in the material. Analytical techniques used to determine the presence and content of carbon include Raman spectroscopy and combustion analysis. These results are presented in the following subsections:

Micro-Raman spectroscopic data recorded with the help of Prof. George Wolf, Arizona State University and was primarily used to analyze the bonding character and particularly the nature of the carbon inclusions. Powders annealed above 1400 °C are mixtures of white and black particles. The probe resolution of the Raman instrument was small enough to acquire spectra from individual particles, which confirmed that black particles contained carbon while white particles did not and, furthermore, in both cases, the spectral features confirmed that the material was predominantly amorphous (Figure 20).

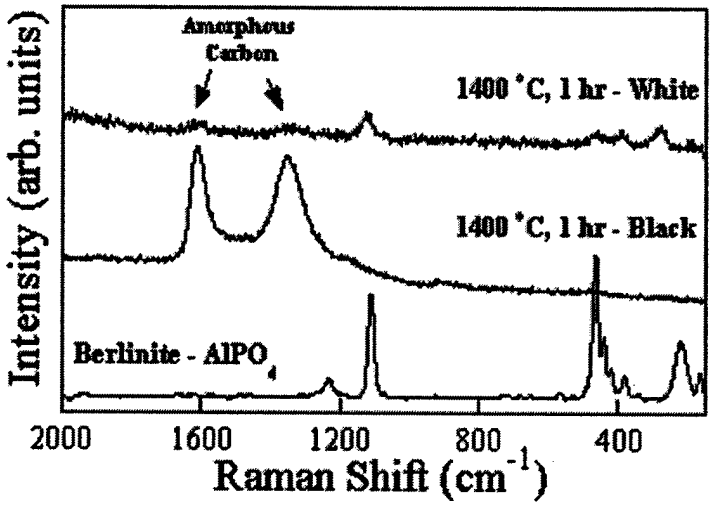

Figure 20. HV depolarized Micro-Raman Spectra acquired at $\lambda = 514$ nm with backscattering configuration (50X Mititoya objective) and spatial resolution of < 5 μm.

The black particles showed peaks at 1350 and 1600 cm^{-1} assignable to amorphous carbon [18]. White particles showed weak broad signals corresponding to both amorphous content and disordered domains of nanocrystalline $AlPO_4$ [19]. Raman spectrum of Berlinite-$AlPO_4$ is also included in the figure for comparison which shows relatively intense and sharp Raman peaks due to crystalline nature.

The carbon content of several samples was also determined using standard combustion techniques. Values are listed in Table 3. The instrument was calibrated with acetanilide as the standard. Samples from six different preparations using the same parameters had an average carbon content of 4.98 wt%.

Table 3. Carbon contents for powders annealed to 1100 °C, 1 h.

Sample No.	Carbon Content (wt%)
1	4.10
2	5.19
3	5.19
4	5.04
5	4.21
6	6.12

D. Doped Cerablak™ Materials via Precursor Modification

The precursor chemistry of Cerablak™ can be modified by adding other metal ions. The suitable additions can be used to tailor thermal, optical, chemical, electrical, and mechanical properties. The thermal stability and film forming abilities can also improved by the addition of suitable elements. The powder XRD pattern of material derived from the pyrolysis of doped Cerablak™ at 1100 °C showed (Figure 21) the material to be completely amorphous without any Bragg peaks.

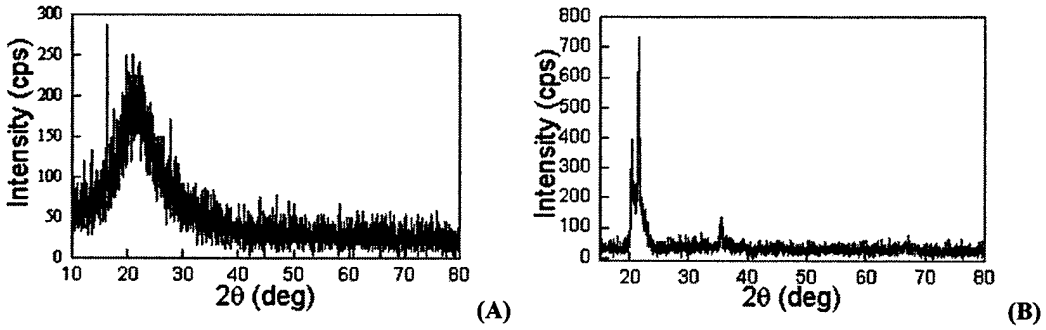

Figure 21. Powder XRD patterns of samples heated at 1100 °C for 1 h (A) Doped Cerablak™ and (B) Undoped Cerablak™

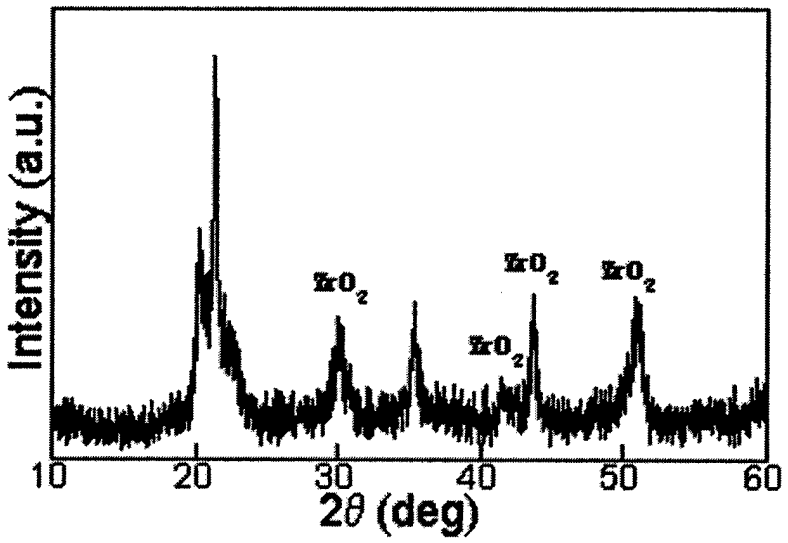

Figure 22. Powder XRD pattern of Cerablak/Zr composite

The nanocomposites with a variety of oxides such as SiO_2, ZrO_2, $ErPO_4$, TiO_2 are obtained by adding corresponding metal salts or organometallics in the precursor solutions and pyrolysing the mixture (Figure 22). There are two routes to the formation of Cerablak™ nanocomposites: *in-situ* and *ex-situ*. *In-situ* formation of nanoparticles avoids the problems associated with the handling of dry nanopowders. *In-situ*-formed oxide nanocrystals have been demonstrated in Cerablak™: ZrO_2 (5 - 50 nm), $ErPO_4$ (10 - 100 nm), $CaWO_4$, Al_2O_3, $AlPO_4$ (5 - 100 nm), and TiO_2. Additionally, due to the very low oxygen diffusivity of Cerablak™, it is believed that composites containing nanocrystalline metals are also possible through the use of microemulsion techniques. For *ex-situ* nanopowders, a wide variety of carbides, chalcogenides, nitrides, oxides,

and metals can be dispersed in the alcoholic precursor to be encapsulated in the final product.

Cerablak™ offers a highly stable matrix for the formation and encapsulation of nanoparticles to result in nanocomposite materials. One of the most surprising is the existence of a Cerablak™-carbon nanocomposite. The addition of Zr^{4+} or Er^{3+}, along with appropriate precursor and annealing treatments, yield ZrO_2 or $ErPO_4$ nanocomposites, respectively, shown in Figure 23A and B. The precursor solution chemistry can also be varied to create $AlPO_4$ nanocomposites.

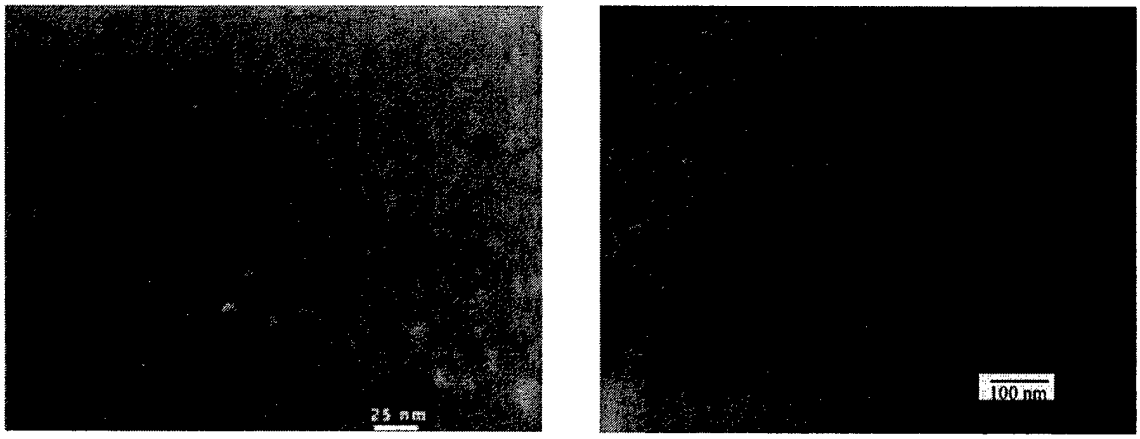

(A) (B)

Figure 23. TEM micrographs of demonstrated Cerablak™ nanocomposites (A) Cerablak™ -ZrO_2 nanocomposite. (B) Cerablak™ -$ErPO_4$ nanocomposite.

The carbon is in the form of "glassy carbon," loosely-correlated graphitic sheets, and is observed to be present in this oxide material, even after heat treatment at 1200 °C, as shown in Figure 24.

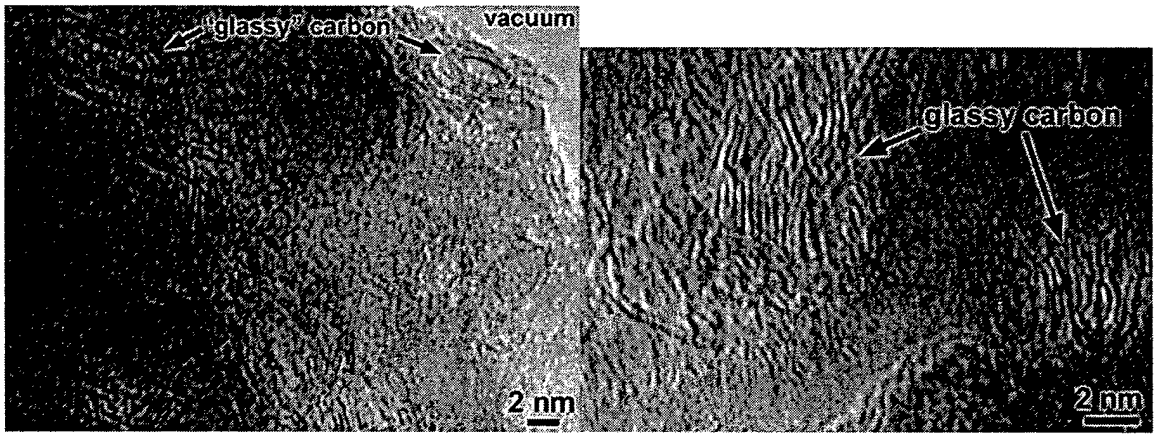

(A) (B)

Figure 24. TEM micrographs of annealed Cerablak™ powders showing nanoinclusions of carbon. A) ethanol precursor and B) butanol precursor.

E. Precursor to High Temperature Material

Based on the characteristics of Cerablak™ precursor solution and the subsequent pyrolyzed product discussed in the previous sections, we can understand the significance of specific aluminum phosphate complexes in yielding high temperature metastable material. Following study on reaction of triethylphosphate ($PO(OC_2H_5)_3$) with aluminum nitrate in ethanol presents the further evidence and best illustration of the correlation between formation of specific aluminum phosphate species and the stability of the corresponding high temperature amorphous aluminophosphates.

Reaction between triethyl phosphate [$PO(OC_2H_5)_3$] and aluminum nitrate in ethanol is investigated. $PO(OC_2H_5)_3$ is a stable chemical and less reactive towards hydrolysis and condensation. So on mixing with aluminum nitrate solution it does not form aluminum phosphate complexes readily unlike mono or diethyl phosphate esters. Figure 25 shows the ^{31}P NMR spectra of $PO(OC_2H_5)_3$ and $Al(NO_3)_3$ mixture in ethanol (2/1 : Al/P) that are (A) un-refluxed and (B) refluxed . It is immediately evident from the ^{31}P NMR spectra that the refluxing action has yielded the P-O-Al type complex species in solution [20]. The un-refluxed solution shows mainly ^{31}P NMR resonance peak corresponding to unreacted $PO(OC_2H_5)_3$ (Figure 25A), and the product obtained by drying and calcining at 1200 °C show formation of highly crystalline cristobalite. (Figure 25C).

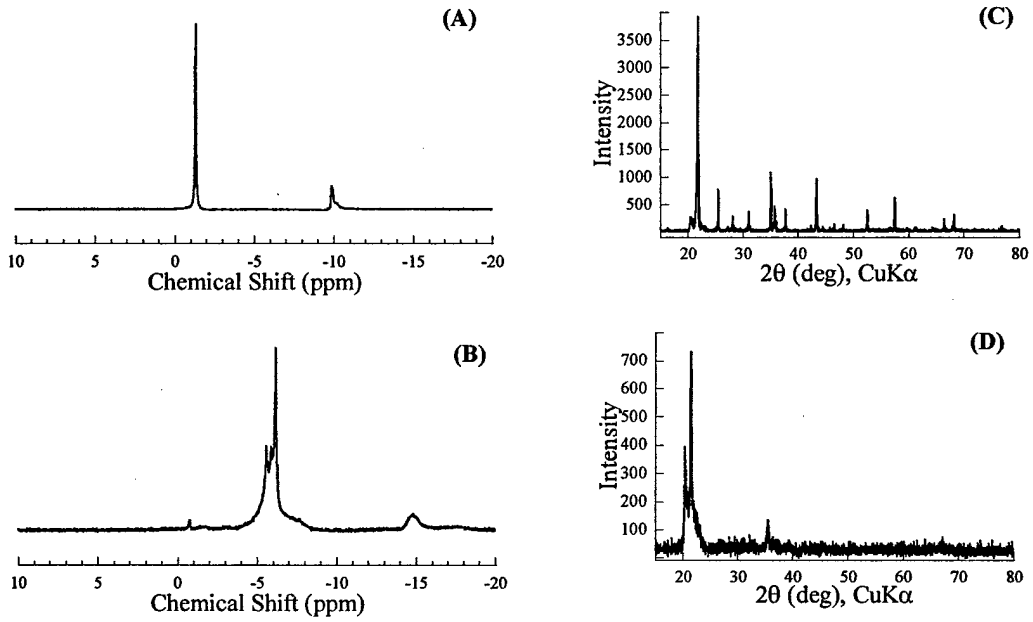

Figure 25. ^{31}P NMR spectra of reaction mixture between $PO(OC_2H_5)_3$ and $Al(NO_3)_3$ in ethanol (A) unrefluxed mixture showing mainly resonance peak for $PO(OC_2H_5)_3$ and (B) refluxed mixture showing resonance peaks centered near -6 ppm, corresponding to aluminophosphate complex (85% H_3PO_4 used as reference). Powder XRD patterns of aluminophosphates calcined at 1200 °C for 50 h, obtained by the pyrolysis of the mixture of $PO(OC_2H_5)_3$ and $Al(NO_3)_3$ in ethanol (C) unrefluxed solution and (D) refluxed solution

A key point is that, in both cases, the solutions are clear with atomic-level mixing, but the results are dramatically different. In the unrefluxed solution, phosphate esters are indeed present, but that does not yield the amorphous material. The refluxing action promotes the formation of phosphate ester complexes that incorporate Al-O-Al, which then yields the amorphous product. Thus both requirements of a) $(OR)_xP=O$ and b) Al-O-Al to be part of a cluster unit seem to be important. This trend is consistently observed with a number of other synthetic routes [21]. The species common to all solutions that yield amorphous materials stable above 1000 °C are those consisting of at least [O=P-O-Al-O-Al] links.

Studying the evolution of the amorphous solid from the gel state also provides interesting insights. Upon pyrolysis, cross-linking of [O=P-O-Al-O-Al] moieties continue over a range of temperatures eventually resulting in a "[-PO_4-AlO_4-AlO_6-AlO_4-PO_4-]" fragment in the high-temperature amorphous framework. The presence of this type of linkage in the calcined material

is established from combined data of NMR and FTIR spectroscopy. ^{27}Al solid state NMR spectra for $x = 1$, with a prominent peak centered at +39 ppm corresponding to tetrahedral coordination for aluminum, along with a very broad peak centered near +7 ppm which is assigned to a "distorted" octahedral aluminum [22], the intensity of which increases with excess aluminum content. This is unlike the exclusive tetrahedral coordination for aluminum observed in all crystalline polymorphs of $AlPO_4$ [23]. The deconvolution of +39 ppm peak suggests a distorted environment for the tetrahedral Al, whereas the corresponding ^{31}P NMR shows an undistorted environment for $[PO_4]$ groups. From these data, we may supposedly conclude that $[PO_4]$ groups are linked symmetrically to four $[AlO_4]$ groups, which in turn, are linked to $[AlO_6]$ groups.

Based on these observations, one can construct the sequence of events leading to this unique amorphous material. Upon pyrolysis, for $AlPO_4$ to crystallize, $P(OAl)_4$ and $Al(OP)_4$ groups should condense to form a 3-D network. For the crystallization of Al_2O_3 to occur, Al should be coordinated to only -OAl and not to -OP to form $Al(OAl)_6$. Thus, the formation of alternating Al-O-P and Al-O-Al groups in the solid, via the initial [O=P-O-Al-O-Al] cluster, prevents the formation of either alumina or $AlPO_4$ crystals, and thereby stabilizes the amorphous network. Why such chains do not rearrange at high temperatures to form crystalline phases is not fully understood. However, there is strong evidence that the atom mobility or diffusivity in the material is very limited. In fact, powders annealed to 1100 °C are jet black in color and even at 1400 °C, the powders still retain a black or gray color from the presence of nanocrystalline carbon (2-5 nm – 5 wt.%) encapsulated in the amorphous matrix. It appears that the ester group attached to the phosphorous in the precursor is the source for the residual carbon in the solid.

F. Properties of Cerablak™ Materials

a. Physical Properties of Cerablak™

Dielectric Constant	2.2 – 3.6
Thermal Conductivity	1-1.5 W/mK
Refractive Index	1.51
Refractive Index (with dopants)	1.5-1.7
Chemical (Oxygen) diffusivity	1×10^{-9} to1×10^{-10} cm^2/sec
%Transmittance (on Sapphire)	>80% in the range 0.5 - 5 μm
Surface Energy	~32 mJ/m2
Coefficient of Thermal Expansion	5 x 10-6 K-1
Hardness	6-8 Gpa
Emissivity (black slurry coating)	>0.9
Coefficient of Friction	0.1

b. Low Oxygen Diffusivity in Cerablak™

In the present study, indirect chemical diffusivity measurements were performed using carbon as a marker. Although ^{18}O tracer experiments are usually employed to accurately measure self and chemical diffusivities of oxygen in ceramic and glass materials, rough estimates of oxygen chemical diffusivities can be made in this case using carbon as a diffusion marker. It was possible to synthesize Cerablak™ as dense bulk particles (Figure 26) which are black and as they are treated to elevated temperatures, begin to form a white shell on the outside as carbon is lost to the atmosphere as CO/CO_2. Figure 26B shows photographs of these particles in which the white boundaries with a black core are readily apparent.

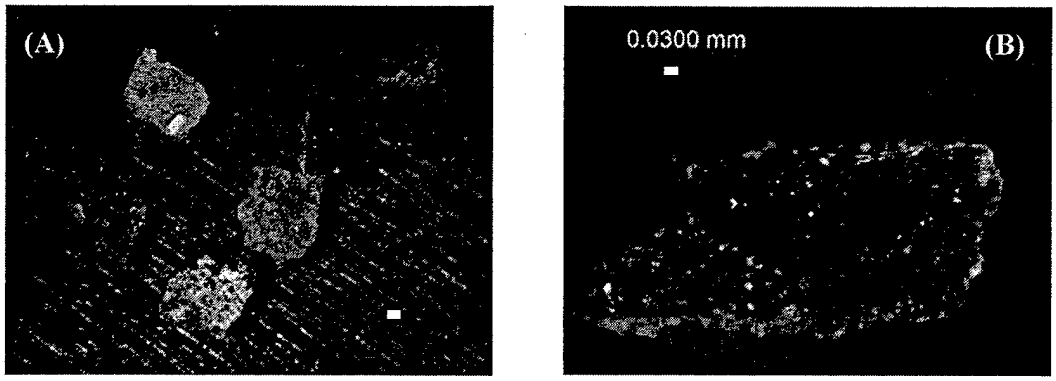

Figure 26. (A) Photographs of dense Cerablak™ particles after high temperature treatment showing the white outer shells with black inner cores. (B) Magnified view of one of the particles.

Figure 27 shows the SEM micrograph of the particle revealing its dense nature. In most cases, under the optical microscope, extremely planar boundaries are seen separating the white outer region from the black inner region. Thus the width of the white region served as the diffusion length corresponding to the oxygen intake.

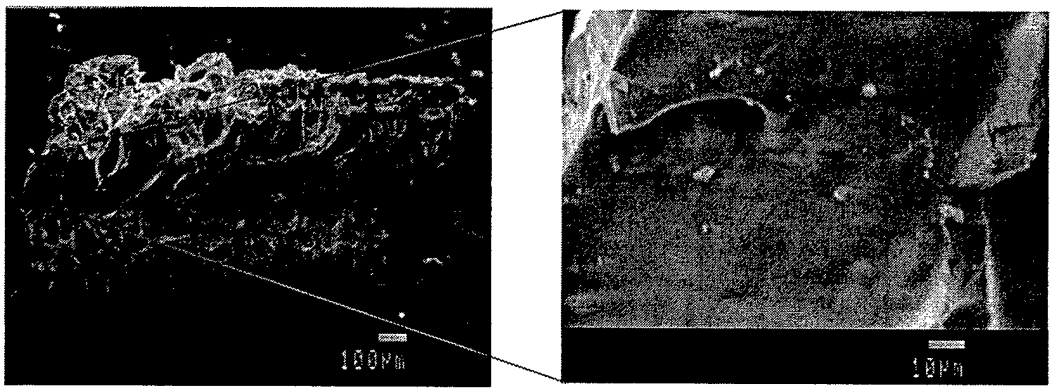

Figure 27. SEM micrographs of Cerablak™ showing the highly dense nature of particles.

Figure 28 shows the diffusivity data for exposures between 1300-1400 °C. The measured diffusion lengths taken under the optical microscope are listed in the table (see inset in Figure 28). Estimated chemical diffusivity values ranged between 1×10^{-9} to1×10^{-10} cm^2/sec which is extremely low and compares favorably with oxygen chemical diffusivities in silica at these temperatures.

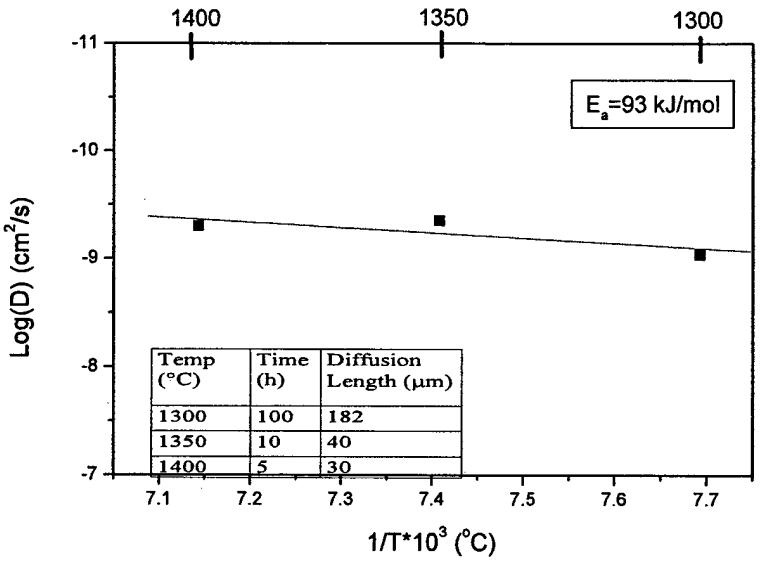

Figure 28. Oxygen diffusivity measurements in Cerablak™ dense powders at 1300-1400 °C, for 5-100 hr. Inset shows the diffusion lengths measured.

c. Refractive Index

Modifying the refractive index and increasing the hardness of the Cerablak™ can be achieved by suitable additions to precursor solution. Refractive index of Cerablak™ can be increased by suitable heavy element addition to the precursor solution. Figure 29 shows the effect of addition of proprietary metal ions in the Cerablak™ solution.

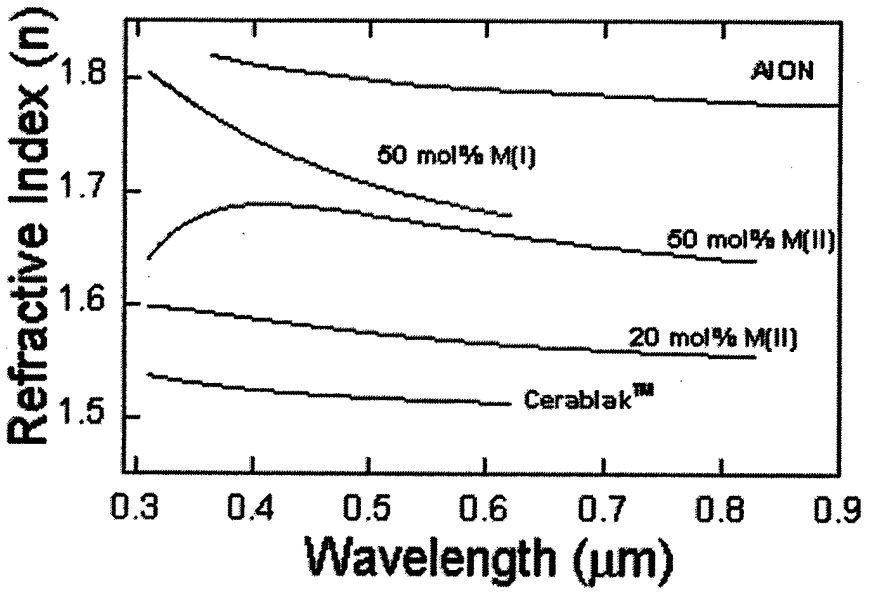

Figure 29. Plot of Refractive index (n) as a function of wavelength.

In Table 5, we give the thickness of the Cerablak™ coating on silicon determined by using ellipsometry. Thickness of the coating can be modified by changing the solution concentration, viscosity, and the withdrawal rate when removing the sample from the solution bath.

Table 5. Refractive Index and Thickness of Cerablak Coatings with Dopants

Material	Thickness (nm)	Refractive Index (n) at Wavelength 589nm
Cerablak™	142	1.51
Cerablak™/50mol% M(I)	89	1.68
Cerablak™/20mol% M(II)	111	1.56
Cerablak™/50mol% M(II)	103	1.66

d. Cerablak™ in high temperature, high pressure steam

A dense piece of electroconsolidated-Cerablak™ was sent to Oak Ridge National Lab for testing in their Kaiser rig. The Kaiser rig runs at 1200 °C for 500 hours, with a total pressure of 10 atm, 15% of which is steam. The piece was weighed before and after the test, and lost only a small amount of weight (4.9%). This weight loss is commensurate with the carbon content in the original pellet (~5%). The piece was completely white, but still intact and sturdy (Figure 30).

X-ray diffraction of the surface showed crystalline alumina and Cerablak™ (Figure 31). Energy dispersive spectral analysis (EDS) of the surface showed only aluminum, no phosphorous. 150 microns was removed from the surface with silicon carbide paper polishing. The XRD pattern of the polished sample showed predominately the presence of Cerablak™, with very weak alumina peaks (Figure 31B). This surface was almost completely white, but showed a few black particles embedded in the white matrix. This result is significant not only that is shows Cerablak™ is stable in high temperature, high pressure steam, but also because it shows that Cerablak™ can turn white without completely turning to crystalline alumina and crystalline aluminum phosphate.

Figure 30. Photograph of section of Cerablak pellet not exposed to the Kaiser rig conditions (above), with pellet exposed to the Kaiser rig (below).

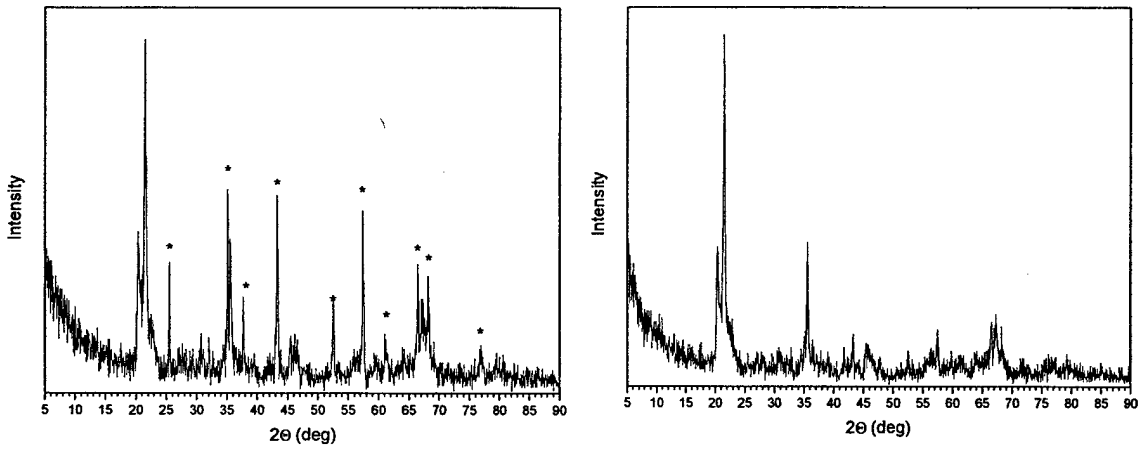

(A) (B)

Figure 31. XRD pattern of Cerablak™ pellet after 500 hours at 1100 °C in 10 atm pressure, with 15% steam. a) original surface of pellet (starred peaks indicate corundum). b) Surface after removal of 150 μm top surface.

e. Optical Properties of Cerablak™

Cerablak™ shows high transmittance between 3 – 5 μm midwave window as well as in the visible region of the electromagnetic spectrum. Cerablak™ coatings were deposited on sapphire, and the transmission properties were measured and compared to an uncoated sapphire piece. Figure 32A shows the transmission of the coated vs. uncoated sapphire plates.

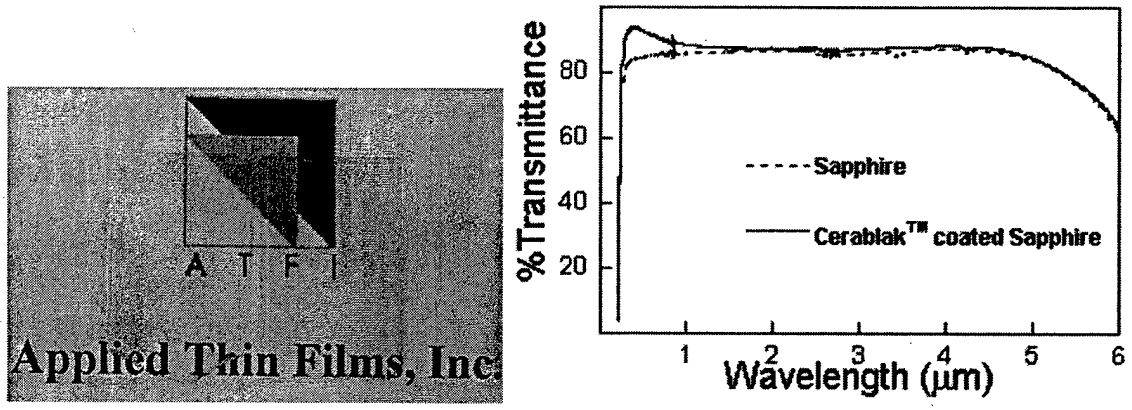

(A) (B)

Figure 32. (A) Photograph of Cerablak™ coating on sapphire, showing its excellent smoothness and transparency. (B) Transmission spectra of Cerablak™-coated sapphire and uncoated sapphire showing Cerablak™'s transmittance property.

f. Planarization effect

Previous studies have shown the oxidation and corrosion protection ability of Cerablak™ coatings. For most of these applications, the surfaces of the substrate materials are relatively rough and they contain relatively high levels of porosity. The pores in the bulk are helpful in imparting toughness to the ceramic material, however, they also serve as channels for diffusion of gases and other liquids which cause material degradation, especially in harsh environments and at elevated temperatures. For many applications, decreasing surface roughness may be important. Cerablak™ can be coated on polished or unpolished surfaces. In both cases, Cerablak™ coating planarizes coated surface leaving a hermetic, extremely smooth layer after curing. Cerablak™ coatings can also be used to seal defects on the surface of an alloy substrate. Transmission electron microscopy showed that the Cerablak™ coating is microstructurally dense, hermetic, and smooth. The transmission electron micrograph of Cerablak™ coated on the type 304 stainless steel shown in Figure 33 illustrates the planarization effect and lack of pinholes or defects in the coating, as well as the amorphous character.

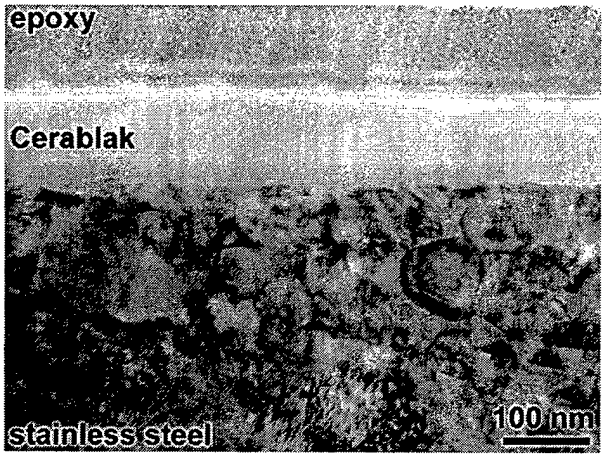

Figure 33. TEM image of Cerablak™ coated on stainless steel SS304 substrate. Epoxy is used as embedding matrix.

Planarization effect is convincingly illustrated by surface roughness (rms) values using atomic force microscopy (AFM) before and after Cerablak™ coating on Inconel substrate (Figure 34) Surface roughness is decreased by 4X after Cerablak™ coating.

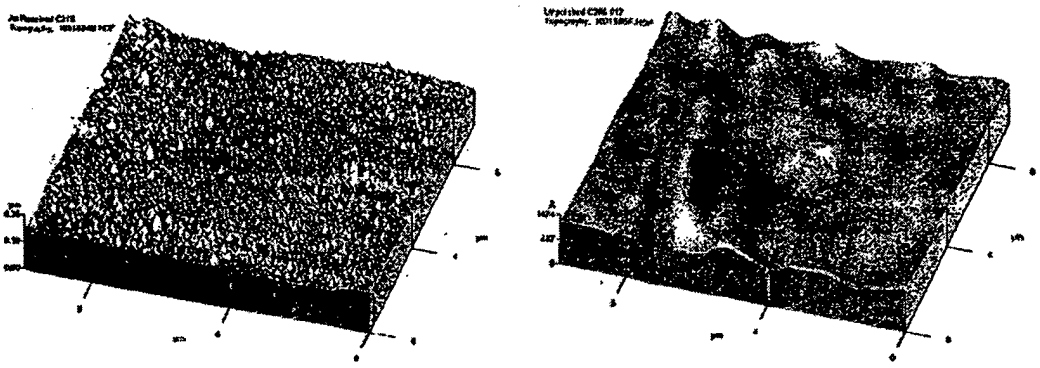

Figure 34. AFM images with rms values of uncoated and Cerablak™ coated Inconel surfaces

This effect is also observed in coatings on ceramic substrates. A piece of unglazed ceramic floor tile was coated with Cerablak™ . The sample is cured 500°C to remove the organics and nitrates and form a fully inorganic film. The coating has filled in the small pores and reduced the surface roughness on the microscale, while the large scale (>10μm) surface roughness is unaffected, leaving the non-skid properties of the tile intact (Figure 35).

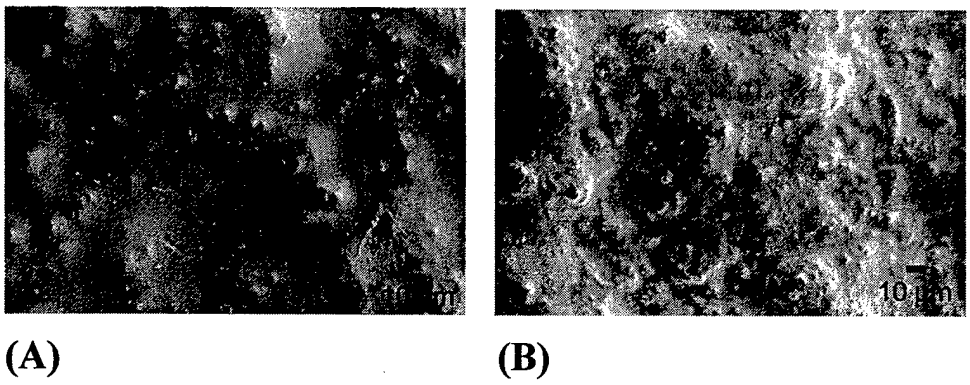

Figure 35. SEM micrographs showing (A) Cerablak™ coated and (B) uncoated unglazed ceramic tile

III. TECHNOLOGY DEVELOPMENT OF AMORPHOUS ALUMINUM PHOSPHATE

Technological applications of Cerablak™ can be derived from various forms like monoliths, microsized powders, films, coatings, fibers, and composites obtained from the precursor solution. These are combined with compositional and microstructural control and low processing temperatures to enhance the potential of Cerablak™ on variety of commercial and military applications. Major part of Cerablak™ technology development under this project is focused on its use as a thin films on hard substrates such metals, glass and ceramics. Surface modification of metals/alloys, glasses, and ceramics, via deposition of thin films, has enabled generation of numerous products [24]. Among the commonly-known uses are surface passivation for protection against harsh chemical environments and high temperature exposure, electrical and thermal insulation, wear and abrasion resistance, non-stick, non-wetting, surface planarization, and surface-modified biological systems. Thin inorganic films are desired due to their inherent hardness and durability and to serve many high temperature applications. Developing pin-hole free, thin and thermally stable inorganic films using low-cost solution-based stable precursor solutions has been a long-standing challenge for material scientists. Despite extensive R&D efforts, inorganic thin films or coatings utilized currently for passivation perform poorly due to inadequate and non-uniform coverage, cracking and spallation, microstructural instability at elevated temperatures, and environmental degradation. Ideally, thin and hermetic inorganic 'glassy' films are desired as they tend to contain lower defect densities and are void of grain boundaries which serve as short circuit diffusion paths. Most inorganic glassy films crystallize at relatively low temperatures (below 800°C), and in addition, stresses induced from phase transformation lead to film cracking and spallation. Hermetic or pin-hole free coverage is a critical requirement even for many low temperature applications, such as atmospheric corrosion protection. While vapor-based deposition processes can produce such high quality dense films, their commercial use is limited to applications where the relatively high cost of capital equipment and processing can be justified for certain products, such as for some microelectronic or optical components. In addition, vapor-based processes do not offer ease of scalability and versatility and cannot be applied in the field as desired for many applications.

As discussed in previous chapters Cerablak™ possesses high temperature amorphous metastability along with a suitable solution-based low-cost process for deposition of thin hermetic films. These aspects of Cerablak™ holds significant promise for a broad range of applications including durable passivation of metal/alloy surfaces. A nominal one micron (or less) thick hermetic film deposited using simple dip-coating or spray or other methods has demonstrated excellent protection against high temperature oxidation and atmospheric corrosion. Coating thickness and drying rate affects the gel formation. When the drying rate is low or the coating is thick, reactions that lead to gelation occur quicker than evaporation, and the coating gels before it dries. Large amount of solvent gets trapped in this gel and leaves porous coating on drying due to the evolution of solvent molecules. In the case of Cerablak™, coating is thin and drying is faster than gel formation. So, the amount solvent trapped in the gel is less and consequently the coating is hermetic or less porous when drying is complete. In metal alkoxide sol-gel chemistry under these conditions the gel formation is incomplete and the film formed is not uniform and continuous on complete drying. In Cerablak™ the polymeric nature of solution also helps in formation of gel with fewer amounts of condensation reactions.

Due to its extremely low oxygen diffusivity and the hermetic nature, ultra-thin films are sufficient to provide the necessary protection in many cases. Film stability under thermal cycling conditions is critically important for many applications and the thin nature of these films will help to minimize the residual thermal stresses such that cracking and spallation is prevented. In addition, these films offer suitable non-stick, non-wetting, and surface planarization characteristics which are critically needed for many industrial, consumer, and military applications. Thus, it is the combination of various attributes of this new development that lends to practical use and places it in a special class of materials with broad commercial potential. We provide a detailed description its high temperature protection and other applications.

Under this project much of Cerablak™ coating is focused on glass substrates. Organic coatings applied directly to soda-lime glass surfaces are effective only under mild conditions in providing low coefficients of kinetic friction and damage protection. Protection under harsh service conditions is feasible if the glass surfaces are sodium-free and contain a hydrophobic organic

overlayer [25]. Thus, glass surface protection and low coefficients of kinetic friction can be accomplished by applying a durable organic overlayer. In such coating systems, Cerablak™ coating functions as an anchor or primer to more firmly bond organic compounds. Organic molecules interact only weakly with soda-lime-silica surfaces. The weakness of the interaction is due to the absence of Lewis acid sites and the weakness of Brönsted acid sites (Si-OH groups) present on glass surfaces. Soda lime-silica surfaces contain mobile sodium ions, which disrupt the bonding between organic adsorbents and glass surfaces and poison Brönsted acid sites required for organic molecule adsorption (alkali-ion weakening effect). Further, under humid conditions, sodium ions diffuse to the surface of the glass and interact with organic molecules resulting in degradation or loss of hydrophobic property. Cerablak™ coating can avoid such type of undesirable chemical events by preventing sodium diffusion to the surface. Furthermore, synergetic effects of organic compounds and Cerablak™ coatings can impart increased hydrophobicity to the glass surface.

Chemical nature of Cerablak™ surface is not yet well understood. However, adsorption of air-borne organics and resulting hydrophobic nature, suggests the presence of active adsorption sites on the Cerablak™ surface. These sites can be attributed to the presence of unsaturated aluminum ions (three or less coordinated) formed by dehydroxylation at higher temperature. It is not unusual that the adsorbed air-borne organics makes the Cerablak™ surface hydrophobic. Similar behavior has been observed for glass and metal oxide surfaces [26]. However, the surprising and unique fact is that the contact angle can be increased as high as 98° by organic adsorption in ambient atmospheric conditions and hydrophobic coating is very stable and durable toward chemical, thermal, and mechanical treatments. Cerablak™ surface possess Al-O-Al and Al-O-P bridges, resulting from the pyrolysis of the precursor solution, which render the surfaces highly reactive. Molecular water, alcohol, acetone or ether can dissociatively adsorb on these sites upon atmospheric exposure resulting in Al-OH and P-OH acidic groups. Thus, both Lewis and Brönsted acids on the Cerablak™ surface are available for organic amphiphilic molecules adsorption which can subsequently make the coated surface highly hydrophobic.

A variety of hydrophobic organic amphiphilic molecules can be self-adsorbed and spontaneously organized on the Cerablak™ surface. The effectiveness of a deposited or adsorbed organic

molecule in protecting the surface and imparting hydrophobicity depends on various factors including strength of adhesion, the length of the alkyl chain, thickness of the organic layer, the extent of intermolecular forces between molecules and the resultant surface energy of the coated surface.

Table 5. Contact angles as function of heat treatment

Slide	25 C	After 20 min heat treatment		
		200 C	300 C	400 C
Cerablak coated	69/70	62/63	34/34	12/10
Cerablak coated	64/64	57/56	37/36	14/16
Cerablak coated	87/87	57/56	38/35	16/12
Cerablak coated	64/64	66/65	39/40	10/5
Cerablak coated	91/92	84/84	52/52	14/11
Uncoated	37/35	42/39	20/21	22/20

We do not have the control over type or ordering of organic molecular adsorption on the Cerablak™ surface from air. But we can control and improve the hydrophobicity of the organic coating over Cerablak™ surface by selecting suitable hydrophobic molecules from a vast class of known organic compounds.

Surface modification techniques have been the focus of research and technology for a variety of applications, including chromatography, wetting and adhesion, lubricants, pigments sensors, and optical and electronic devices. Certain organic molecules in a dilute solution will spontaneously adsorb and organize onto a solid substrate to form a so called 'self-assembled monolayer' (SAM). This process is driven by the interaction of the head-group with the substrate. Most well studied SAMs are heteroepitaxial thiolates (R-SH) on crystalline gold or other metal substrates. The long chain n-alkyl carboxylic acids on alumina and calcium phosphate are also reported. The strength of adhesion of organic molecules to oxide surfaces increases in the order paraffins < fatty alcohols < fatty acids < perfluoro compounds < amines. The chain length of molecules less than 12 carbon atoms behave like liquids and do not self-assemble in forming a hydrophobic layer [27]. Molecules with carbon atoms between 12 and 15, though self-organize to form monolayer of organic sheet and possess limited stability.

Molecules with greater than 16 carbon atoms behave like solids and form highly stable hydrophobic layers and thus are suitable as organic coatings (monolayers). Presence of alkyl groups at the surface of organic layers imparts the hydrophobic property. Among the various organic compounds, long alkyl chain fatty acids are highly hydrophobic, especially oleic acid with 18 carbon alkyl chain. Further, oleic acid molecules with the presence of both carboxylate groups and double bonds can interact with the oxide surface strongly and form close-packed mono-layer with strong intermolecular forces.

Oleic acid and sodium oleate adsorption on soda-lime silicate glasses and calcium minerals such as fluorite, apatite, dolomite, and scheelite have been studied extensively [28]. Based on these studies, it is recognized that the nature of the adsorbed oleic acid molecules and the structure of the adsorbed layer have a major influence on the hydrophobic nature of the outer-layer, which in turn depends on the interaction between oleic acid molecules and oxide surfaces. At present, various mechanisms have been proposed for adsorption of organic molecule on oxide surfaces, namely, physical or electrostatic interactions, chemisorption and surface precipitation. In the case of Cerablak™, Al-OH and P-OH groups present on the surface can interact with oleic acid molecules electrostatically through physisorption at lower concentrations as well as form strong chemical bond with aluminum (Al-OOCR) through chemisorption at higher concentrations. Acidic P-OH groups can also be used in anchoring amines with long alkyl chains (> C18) such as octadecyl amine as an alternative organic overlayer.

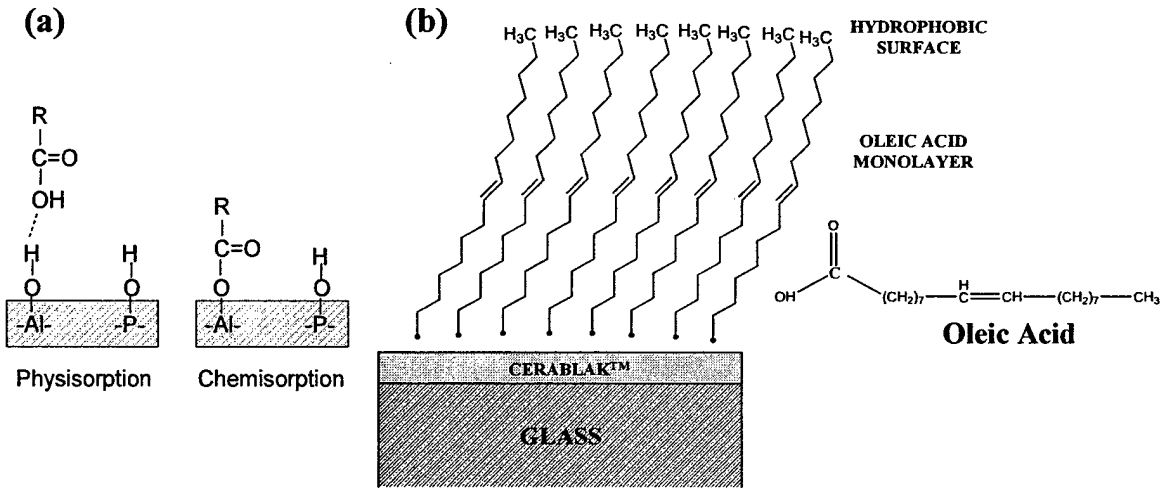

Figure 36. Schematic depiction of a) Physisorption vs. chemisorption and b) Oleic acid on Cerablak coated glass.

Another important class of SAMs is formed by silylation with functional organosilanes of the general formula R_nSiX_{4-n} where X is a readily hydrolyzable group. (most often chloro or alkoxy) on substrates like silica and silicate glasses. *(Silylation is the displacement of an active hydrogen ion (usually in a hydroxyl group) by an organosilyl group).* Hydroxylated substrates such as silicon with a layer of native oxide on the surface, or glass, are then coated by simple immersion in alkylsilane solution for a specified period of time and at a specified temperature. The coated substrates are then typically rinsed to removed weakly bound polymer (often mechanical cleaning (with a camel brush) is also applied) and allowed to "cure" at room temperature or around 100-200 °C of 12-24 hours. Completed SAMs prepared from trichlorosilanes contain no chlorine. The signature of a "high quality alkyl SAM" includes a film thickness of close to the fully extended length of the monomer units and a small average tilt of the tails from the surface normal. (for octadecyltrichlorosilane (OTS) monolayer thickness is ~20Å).

In aluminophosphate surfaces there two chemically distinct active sites are present. Al-OH and P-OH. The presence of both of these groups on the surface of $AlPO_4$ has previously been

confirmed using FTIR spectroscopy. (3800 and 3680 cm^{-1} respectively). Both groups are known to react with silanes (dichlorodimethylsilane) forming strong Al-O-Si and P-O-Si bonds and confirmed by ^{29}Si NMR. It will be interesting to extend this study to incorporate reactions of silanes containing long alkyl chains such as OTS. The general expected reaction scheme is as follows:

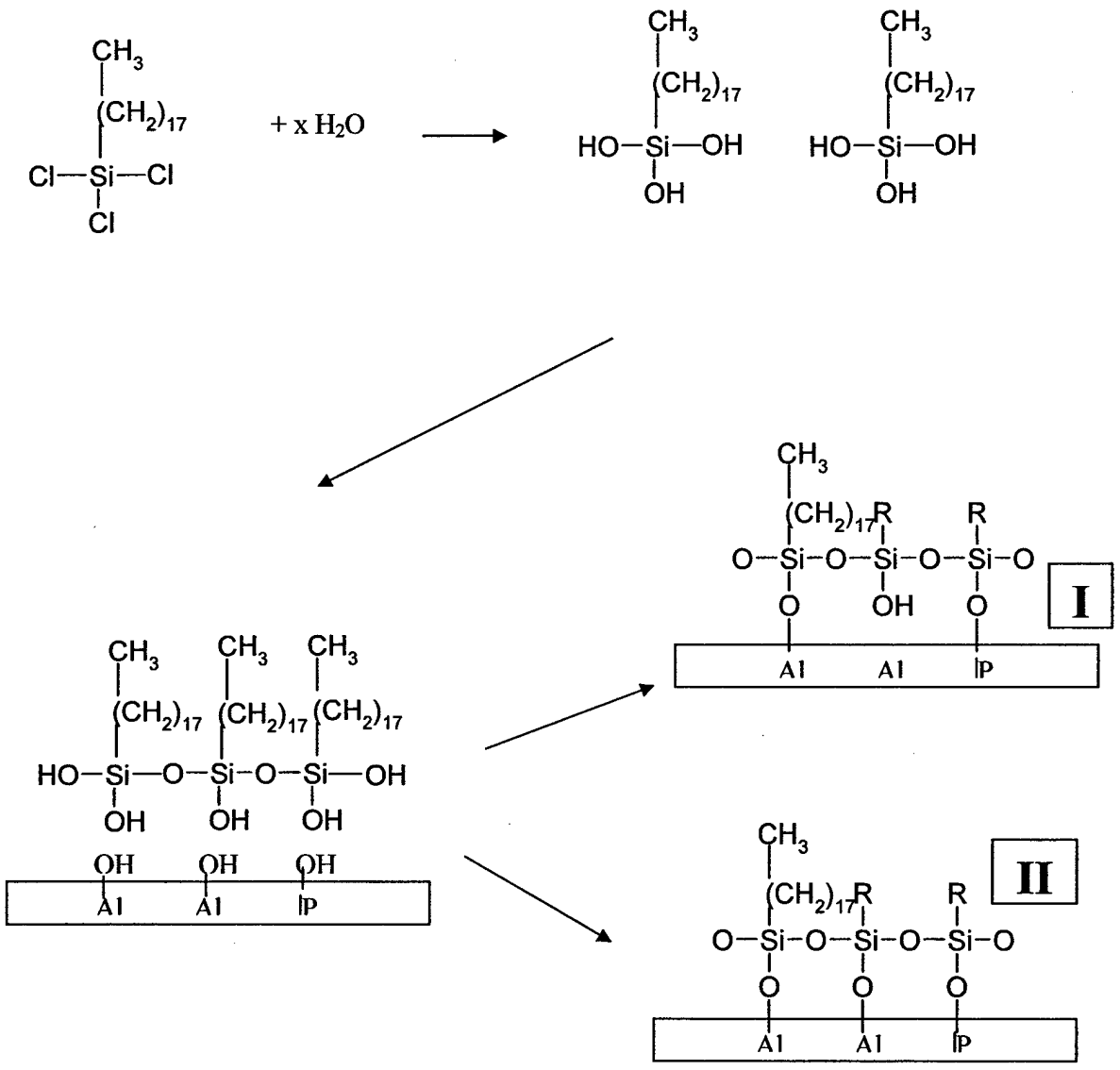

I and **II** are some of the possible bonding configurations. This is strongly depends on the concentration of P-OH and Al-OH groups and Al-Al or Al-P or P-P distances on the surface.

The formation of high quality SAMs depends on several factors (a) reactivity of Al-OH and P-OH (b) distance between two surface OH groups (c) No. of reactive surface –OH groups. Figure 37 shows the thermal stability of silane SAMs on Cerablak™ surface. The stability is followed by heating the Glass/Cerablak/Silane SAMs in an oven at various temperatures up to 200 °C for a period of time and recording the contact angle for water. The photographs clearly show that the silane layers are retained even after 200 °C heat treatment.

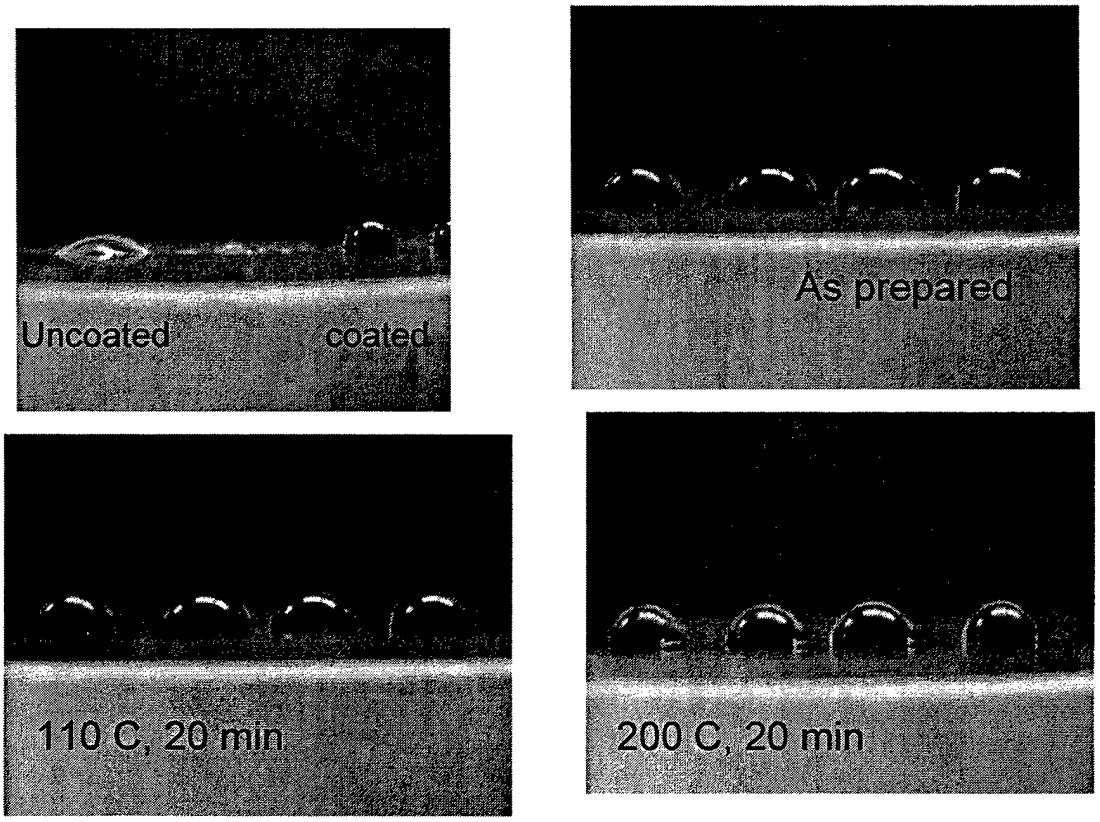

Figure 37. Photographs of water droplets on Cerablak/Silane coated surfaces as function of temperature

References

[1] H. Schroeder, Physics of Thin Films, 87 (1969).

[2]. G. Marcelin, R.F. Vogel, H.E. Swift,T.P. *J. Catal.* 83, 42 (1993).

[3]. Weber, C.; Field, R.; Hoefer, H. H. *Key Engineering Materials*, **150**, 199, (1998).

[4]. G.D. Wignall, R.N. Rothon. G.W. Longman, G.R. Woodward, *J. Mater. Science*, **12**, 1039, (1977).

[5]. L. Coury, F. Babonneau, M. Henry and J. Livage *C.R. Acad. Sci. Paris II* **309**, 799 (1989).

[6]. S. Sambasivan, US Patent No.

[7]. F.A. Cotton, G. Wilkinson, *Advanced Inorganic Chemistry*, 5 ed. pp. 400 John Wiley (1988)

[8]. R.F. Mortlock, A.T. Bell, and C.J. Radke, P-31 And Al-27 NMR Investigations Of Highly Acidic, Aqueous-Solutions Containing Aluminum And Phosphorus, *Journal of Physical Chemistry*, 1993, 97: 767-774.

[9]. K. Okada, C. Aoki, T. Ban, S. Hayashi, A. Yasumori, Effect of Aging Temperature on the Structure of Mullite Precursors Prepared from Tetraethoxysilane and Aluminum Nitrate in Ethanol Solution, *Journal of Europian Ceramic Society*, **16**,149-153 (1996).

[10]. A.F. Ali, P. Mustarelli, A. Magistris, Optimal Synthesis of Organo-Phosphate Precursors for Sol-Gel Preparations, *Materials Research Bulletin*, **33**, 697-710 (1998).

[11]. K. Okada, C. Aoki, T. Ban, S. Hayashi, A. Yasumori, Effect of Aging Temperature on the Structure of Mullite Precursors Prepared from Tetraethoxysilane and Aluminum Nitrate in Ethanol Solution, *Journal of Europian Ceramic Society*, **16**,149-153 (1996).

[12]. A.F. Ali, P. Mustarelli, A. Magistris, Optimal Synthesis of Organo-Phosphate Precursors for Sol-Gel Preparations, *Materials Research Bulletin*, **33**, 697-710 (1998).

[13]. H. Graetsch, H. Gies, I. Topalović, *Phys. Chem. Minerals,* **21,** 166 (1994).

[14]. J.M. Elzea, S.B. Rice, *Clays and Clay Minerals*, **44**, 492 (1996).

[15]. V. Petkov, K.K. Rangan, M.G. Kanatzidis, and S.J.L Billinge *Mat. Res. Soc. Symp. Proc.* **678**, EE1.5.1 (2001).

[16]. G.D. Wignall, R.N. Rothon, G.W. Longman, G.R. Woodward, *J. Mater. Sci.* 12, 1039 (1977)

[17]. R. Dupree, M.H. Lewis, M.E. Smith, *J. Appl. Cryst.* **21**, 109, (1988).

[18]. (a) A.C. Ferrari, J. Robertson, *Phy. Rev. B*, **64**, 75414-1, (2001). (b) D.R. Tallant, T.A. Friedmann, N.A. Missert, M.P. Siegal, J.P. Sullivan, *Materials Research Society Symposium Proceedings* (1998), 498 (Covalently Bonded Disordered Thin-Film Materials), 37-48.

[19]. (a) L.K. Teh, W.K. Choi, L.K. Bera, W.K. Chim, *Solid-State Electronics*, **45,** 1963, (2001).

(b)J.H.D. da Silva, S.W. da Silva, J.C. Galzerani, *J. Applied Phy.,* **77,** 4044, (1995)

[20]. J. Livage, P. Barboux, M.T. Vandenborre, C. Schmutz, F. Taulelle, Sol-Gel Synthesis of Phosphates, Journal Non-Crystalline Solids, 1992,147&148:18-23.

[21]. For example, amorphous products obtained from the precursor solutions containing $H_3PO_4/Al(NO_3)_3$ and $POCl_3/Al(NO_3)_3$ mixture crystallized to cristobalite $AlPO_4$ and α-alumina at 800 °C. Precursor solutions prepared by dissolving P_2O_5 and $Al(NO_3)_3$ in methanol, 2-propanol and 1-butanol resulted in highly stable amorphous materials.

[22]. T.T.P. Cheung, K.W. Willcox, M. P. McDaniel, M.M. Johnson, *J. Catal.*, **102**, 10, (1986).

[23]. T. Apih, U. Mikac, A.V. Kityk, R. Blinc, *Phys. Rev. B,* **55,** 2693 (1997).
[24].M. Ohring, *Material science of thin films,* 2 ed. Academic Press (2001).
[25]. Smay, G.L. *Glass Technology,* **26,** 46 (1985).
[26]. Allara, D.L., Nuzzo, R.G. *Langmuir,* **1,** 45, (1985).
[27]. (a) Timmons, C.O., Zisman, W.A., *J. Phys. Chem.* **69,** 984, (1965), (b) Legaly, G. *Angew. Chem. Int. Ed. Engl.* **15,** 575, (1976).
[28].(a) Mielczarski, J.A. Cases, J.M., Bouquet, E., Barres, O., Delon, J.F. *Langmuir,* **9,** 2370 (1993). (b) Sivamohan, R.; de Donato, P.; Cases, J. M. *Langmuir,* **6,** 637, (1990). (c)Rao, Hanumanth Cases, J. M.; Forssberg, K. S. E. *J. Colloid Interface Sci. 1991, 145, 330.*